

Linear Scaling Electronic Structure Methods

Stefan Goedecker,
Max-Planck Institute for Solid State Research,
Stuttgart, Germany
goedeck@prr.mpi-stuttgart.mpg.de

September 2, 2018

Methods exhibiting linear scaling with respect to the size of the system, so called $O(N)$ methods, are an essential tool for the calculation of the electronic structure of large systems containing many atoms. They are based on algorithms which take advantage of the decay properties of the density matrix. In this article the physical decay properties of the density matrix will first be studied for both metals and insulators. Several strategies to construct $O(N)$ algorithms will then be presented and critically examined. Some issues which are relevant only for self-consistent $O(N)$ methods, such as the calculation of the Hartree potential and mixing issues, will also be discussed. Finally some typical applications of $O(N)$ methods are briefly described.

Contents

1	Introduction	3
2	Locality in Quantum Mechanics	5
3	Basic strategies for $O(N)$ scaling	16
3.1	The Fermi Operator Expansion	19
3.1.1	The Chebychev Fermi Operator Expansion	19
3.1.2	The Rational Fermi Operator Expansion	26
3.2	The Fermi Operator Projection Method	28
3.3	The Divide and Conquer method	28
3.4	The Density Matrix Minimization approach	31
3.5	The Orbital Minimization approach	36
3.6	The Optimal Basis Density Matrix Minimization method	40
4	Comparison of the basic methods	42
4.1	Small basis sets	43
4.2	Large basis sets	49
5	Other $O(N)$ methods	50
6	Some further aspects of $O(N)$ methods	52
7	Non-orthogonal basis sets	54
8	The calculation of the selfconsistent potential	57
8.1	The electrostatic potential	57
8.2	The exchange correlation potential	59
9	Obtaining self-consistency	60
10	Applications of $O(N)$ methods	62
11	Conclusions	66
12	Acknowledgments	67
13	Appendix: Decay properties of Fourier transforms	68
14	References	69

1 Introduction

The exact quantum mechanical equations for many-electron systems are highly intricate. Any attempt to solve these equations analytically for real systems is doomed to fail. Numerical methods such as Configuration Interaction based methods (McWeeny 1989, Fulde 1995) or Quantum Monte Carlo methods (Hammond 1994, Nightingale 1998) can in principle solve these many-electron equations but because of the extremely high numerical effort required, their applicability is rather limited in practice.

The bulk of all practical applications is therefore done within various independent-electron approximations such as the Hartree-Fock method (A. Szabo and N. Ostlund 1982), Density Functional methods (R. Parr and W. Yang 1989) or Tight Binding methods (C. Goringe *et al.*, 1997a, Majewski and Vogl 1986). A comparison of the strength of different methods together with a selection of some interesting applications is given by Wimmer (1996). Even these approximate quantum mechanical equations are still fairly complicated and in general not solvable by analytical methods. Finding efficient algorithms to solve the many-electron problem numerically within any of these approximations is imperative for the applicability of quantum mechanics to physics as well as to chemistry and materials science. Due to efforts in the past satisfactory algorithms are now available and computational electronic structure methods are making very important contributions to our understanding of matter at the microscopic level. The 1998 Nobel prize for W. Kohn and J. Pople is a landmark sign of the importance of this approach. Since computational electronic structure methods are used over a very wide spectrum of applications is it hard to summarize their use. A hint of their versatility can be obtained by looking at the fraction of theoretical articles in several solid state and chemistry journals where computational electronic structure methods are used. As can be seen from Table 1 this fraction varies between 11 and 59 %, being 27 % in the two largest journals in solid state physics (PRB) and chemical physics (JCP).

Table 1: The importance of computational electronic structure methods as measured by the number of publications. Listed are the total number of publications, the number of theoretical publications and the number of publications using computational electronic structure methods in the period from January 1997 to September 1988. To determine whether a paper belongs into this last category, it has to contain either of the key words “electronic structure calculation”, “ab initio calculation”, “tight binding calculation” or “density functional calculation”. I thank Dr Wanitschek for providing me with these data.

Journal	total	theoretical	computational
Physical Review B (Condensed Matter)	7924	4629	1263
Journal of chemical physics	4066	2764	754
Theochem	905	856	502
Chemical physics letters	2319	1209	490
International journal of quantum chemistry	609	582	271
Physical review letters	4558	2834	250
Journal of physics: Condensed matter	1774	927	220

Due to the constant increase in computer power and due to algorithmic improvements the importance of computational methods is growing further. Whereas computational methods nowadays mainly supplement experimentally obtained information, they are expected to increasingly supersede this information.

This article will concentrate on recently developed methods that allow us to calculate the total energy within various independent-electron methods for large systems. Practically all physical observables can be obtained from the total energy, for instance in the form of derivatives with respect to certain external parameters. The reason why large systems containing many atoms are accessible with these algorithms is their linear scaling with respect to the number of atoms. In principle linear scaling should also be obtainable for true many-electron methods. For the MP2 method such an algorithms has indeed recently been reported (Ayala and Scuseria, 1998).

Traditional electronic structure algorithms calculate eigenstates associated with discrete energy levels. The reason for this is probably historical since the prediction of these experimentally observed levels was the first big success of quantum mechanics. The disadvantage of this approach is that it leads to a diagonalization problem which has a cubic scaling in the computational effort. Direct diagonalization (Press *et al.*, 1986), which was the standard approach in the early days of the computational electronic structure era, has a cubic scaling with respect to the size of the Hamiltonian matrix, i.e. with respect to the number of basis functions M_b . Iterative diagonalization schemes (Saad 1996), preconditioned conjugate gradient minimizations (Teter *et al.*, 1989, Štich *et al.*, 1989, Payne, *et al.*, 1992) and the Car-Parrinello method (Car and Parrinello 1985) for molecular dynamics simulations were a big algorithmic progress because of their improved scaling behavior. Their scaling was not any more proportional to the cube of the the number of basis functions but grew only like $M_b \log(M_b)$ if plane waves were used as a basis set. Nevertheless these methods still have a cubic scaling with respect to the number of atoms N_{at} , which comes from the orthogonality requirement of the wavefunctions. The reason why this orthogonalization step scales cubically can easily be seen. As the system grows, each wavefunction extends over a larger volume and has therefore to be represented by a larger basis set resulting in a longer vector. At the same time there are more such wavefunctions and each wavefunction has to be orthogonalized to all the others. Thus there are 3 factors that grow linearly, resulting in the postulated cubic behavior. The computer time T_{CPU} required to do the calculation is thus given by

$$T_{CPU} = c_3 N_{at}^3, \quad (1)$$

where c_3 is a prefactor. It has to be pointed out that Equation (1) gives only the asymptotic scaling behavior. Within Density Functional and Hartree Fock calculations there are other terms with a lower scaling which dominate for system sizes of less than a few hundred atoms due to their large prefactor. In the case of plane wave type calculations the Fast Fourier transformations necessary for the application of the potential to the wavefunctions consume most of the computational time for small systems, in the case of calculations using Gaussian type orbitals (Hehre 1996) it is the calculation of the Hartree potential. This cubic scaling is a major bottleneck nowadays since in many problems of practical interest one has to do electronic structure calculations for systems containing many (a few hundred or more) atoms. Evidently, cubic scaling means that if one dou-

bles the number of atoms in the systems the required computer time will increase by a factor of eight. By enlarging the system one therefore rapidly reaches the limits of the most powerful computers. So called $O(N)$ or low complexity algorithms are therefore a logical next step of algorithmic progress since they exhibit linear scaling with respect to the number of atoms

$$T_{CPU} = c_1 N_{at} . \quad (2)$$

These methods offer thus the potential to calculate very large systems. The prefactors c_1 and c_3 depend on the approximation used for the many-electron problem. For a Density Functional calculation with a large basis set the prefactors are of course much larger than for a Tight Binding calculation, where the number of degrees of freedom per atom is much smaller. The prefactor c_1 depends also on what $O(N)$ method is used, but in general the prefactor c_1 is always larger than c_3 assuming that the same independent-electron approximation is used both in the traditional and $O(N)$ version. There is therefore a so called cross over point. For system sizes smaller than the cross over point the traditional cubic scaling algorithms are faster, for larger systems the $O(N)$ methods win. Tight Binding calculations are an ideal test environment for $O(N)$ algorithms. Because of their rather small memory and CPU requirements one can easily treat systems comprising of a very large number of atoms and venture into regions beyond the cross over point. Contrary to what one might naively think, the importance of $O(N)$ algorithms will also increase as computers get faster. Whereas at present it is difficult to access the cross over region situated at some 100 atoms using the Density Functional framework, this will be easy with faster computers and $O(N)$ algorithms will be the algorithms of choice.

Even though $O(N)$ algorithms contain many aspects of mathematics and computer science they have nevertheless deep roots in physics. Obtaining linear scaling is not possible by purely mathematical tricks but it is based on the understanding of the concept of locality in quantum mechanics. Conversely, the need of constructing $O(N)$ algorithms was also an incentive to investigate locality questions more deeply, and has thus lead to a better understanding of this very fundamental concept. An algorithmic description of electronic structure in local terms can give a justification of the well established concepts of bonds and lone electron pairs in empirical chemistry.

Since $O(N)$ algorithms are based on a certain subdivision of a big system into smaller subsystems, techniques developed in this context might also be helpful in reaching another important goal for treating large systems, namely combining electronic structure methods of different accuracy such as empirical Tight Binding and Density Functional theory in a single system.

2 Locality in Quantum Mechanics

Locality in Quantum Mechanics means that the properties of a certain observation region comprising one or a few atoms are only weakly influenced by factors that are spatially far away from this observation region. This fundamental characteristic of insulators is well established within independent-electron theories (Heine 1980) and it can even be carried over into the many-electron framework (Kohn 1964).

Traditional chemistry is based on local concepts. Covalently bonded materials are described in terms of bonds and lone electron pairs. It is standard textbook knowledge that the properties of a bond are mainly determined by its immediate neighborhood. The decisive factors are what type of atoms and how many of them (the coordination number) are surrounding it. Second nearest neighbors and other more distant atoms have a very small influence. As an example let us look at the total energy of a hydrocarbon chain molecule C_nH_{2n+2} . In this case each CH_2 subunit is from an energetical point of view practically an independent unit. As one adds one CH_2 subunit, the energy increases by an amount which is nearly independent of the chain length. Already the insertion of a CH_2 subunit into the smallest chain C_2H_6 gives an energy gain which agrees within 10^{-4} a.u. with the asymptotic value of the insertion energy for very long chains. This means that the electrons belonging to this inserted subunit already do not see any more the end of the chain for very short chain lengths. This example is a drastic illustration of a principle sometimes termed “nearsightedness” (Kohn 1996). In other insulating materials the influence of the neighboring atoms decays slower. An example is shown in Figure (1), where the total energy per silicon atom is plotted as a function of the size of its crystalline environment.

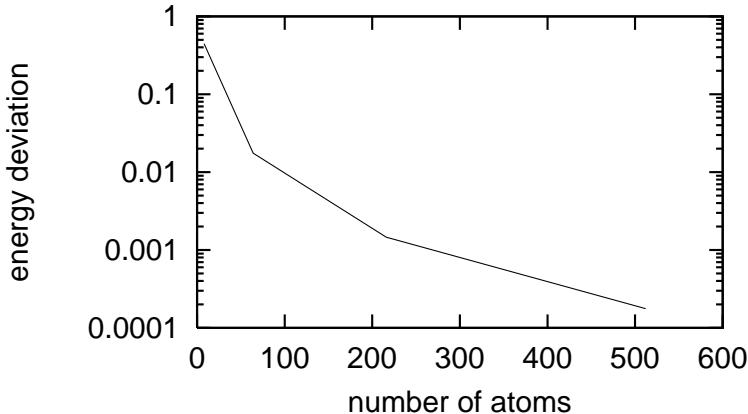


Figure 1: *The deviation of the total energy per silicon atom from its asymptotic bulk value as a function of the size of the periodic volume in which it is embedded. The calculation was done with a Tight Binding scheme using exact diagonalization*

Even in metallic systems, where the elementary bond concept is not any more valid, locality still exists. This is supported by the well known fact, that the total charge density in a metal is given with reasonable accuracy by the superposition of the atomic charge densities. Since atomic charge densities decay rapidly, this implies that the charge density at the midpoint of two neighboring atoms is mainly determined by the two closest atoms and very little by other more distant atoms. Another related example is given by V. Heine (Heine 1980) who points out, that the magnetic moment of an iron atom, which is embedded in an iron-aluminum alloy differs by less than 5 % from the value for pure iron if the atoms are locally surrounded by only eight aluminum atoms.

This locality is not at all reflected in standard electronic structure calculations which are based on eigenorbitals extending over the whole system, making both the interpretation of the results more difficult and requiring unnecessary computational effort. The

simplistic bond concepts of empirical chemistry are certainly not adequate for electronic structure calculations aiming at high accuracy. Nevertheless one might hope to incorporate some more general locality concepts into electronic structure calculation to make them both more intuitive and efficient. In the following we will therefore carefully examine the range of interactions in quantum mechanical systems.

Self-consistent electronic structure methods require essentially two steps. The calculation of the potential from the electronic charge distribution and the determination of the wavefunction for a given potential. In non-self-consistent calculations such as Tight Binding calculations, the first step is not needed.

The calculation of the potential consists usually of two parts, the exchange correlation potential, and the Coulomb potential. The exchange correlation potential is a purely local expression in Density Functional Theory and can therefore be calculated with linear scaling. In the Hartree Fock scheme one might first think that the exchange part is non-local, but a more profound examination reveals (section 8.1) that it is local even in this case. The Coulomb potential on the other hand is very long range and needs proper treatment. A naive evaluation of the potential U arising from a charge distribution ρ by subdividing space into subvolumes ΔV and summing over these subvolumes,

$$U(\mathbf{r}_i) = \sum_j \frac{\rho(\mathbf{r}_j)}{|\mathbf{r}_i - \mathbf{r}_j|} \Delta V,$$

would result in a quadratic scaling since both indices i and j have to run over all grid points in the system. The Coulomb problem actually arises not only in the context of electronic structure calculations but also in classical calculations of coulombic and gravitational systems such as galaxies of stars. Much effort has therefore been invested in this computational problem and several algorithms are known which solve the problem with linear scaling. These methods will be described in section 8.1.

The more interesting and more difficult part is to assess the role of locality for a given external potential. The appropriate quantity to study this property is the density matrix. The one-particle density matrix F completely specifies our quantum mechanical system within the independent electron approximation and all quantities of interest can easily be calculated from it. The central quantities in any electronic structure calculation, the kinetic energy E_{kin} , the potential energy E_{pot} and the electronic charge density ρ are given by

$$E_{kin} = -\frac{1}{2} \int \nabla_{\mathbf{r}}^2 F(\mathbf{r}, \mathbf{r}') \Big|_{\mathbf{r}=\mathbf{r}'} d\mathbf{r}' \quad (3)$$

$$E_{pot} = \int F(\mathbf{r}', \mathbf{r}') U(\mathbf{r}') d\mathbf{r}' \quad (4)$$

$$\rho(\mathbf{r}) = F(\mathbf{r}, \mathbf{r}), \quad (5)$$

where $U(\mathbf{r}')$ is the potential. A related quantity which will frequently be used throughout the article is the band structure energy E_{BS} defined as

$$E_{BS} = E_{kin} + E_{pot} \quad (6)$$

and the grand potential

$$\Omega = E_{BS} - \mu N_{el}, \quad (7)$$

where μ is the chemical potential and N_{el} the number of electrons. Subtracting μN_{el} from E_{BS} leaves Ω invariant under a constant potential offset. If one applies the shift ($U(\mathbf{r}) \rightarrow U(\mathbf{r}) + const$) the potential energy will increase by $N_{el} const$. In order to conserve the total number of electrons, μ also has to be shifted ($\mu \rightarrow \mu + const$) and thus Ω remains constant.

Discretizing the Hamiltonian H which is the sum of the kinetic and potential energy as well as F with respect to a finite orthogonal basis $\phi_i(\mathbf{r})$, $i = 1, \dots, M_b$ one obtains

$$H_{i,j} = \int \phi_i^*(\mathbf{r}) \left(-\frac{1}{2} \nabla_{\mathbf{r}}^2 + U(\mathbf{r}) \right) \phi_j(\mathbf{r}) d\mathbf{r} \quad (8)$$

$$F_{i,j} = \int \int \phi_i^*(\mathbf{r}) F(\mathbf{r}, \mathbf{r}') \phi_j(\mathbf{r}') d\mathbf{r} d\mathbf{r}' \quad (9)$$

and the expressions for the central quantities become

$$E_{BS} = Tr[FH] \quad (10)$$

$$\Omega = Tr[F(H - \mu I)] \quad (11)$$

$$\rho(\mathbf{r}) = \sum_{i,j} F_{i,j} \phi_i(\mathbf{r}) \phi_j(\mathbf{r}), \quad (12)$$

where Tr denotes the trace. It follows from Equation (12) that the total number of electrons N_{el} in the system is given by

$$N_{el} = Tr[F]. \quad (13)$$

Evaluating the traces using the eigenfunctions Ψ_n of the Hamiltonian one obtains immediately the well known expressions for N_{el} , E_{BS} , Ω and ρ within the context of conventional calculations which are based on diagonalization. Denoting the eigenvalues associated with the eigenfunctions Ψ_n by ϵ_n one obtains

$$N_{el} = \sum_n f(\epsilon_n) \quad (14)$$

$$E_{BS} = \sum_n f(\epsilon_n) \epsilon_n \quad (15)$$

$$\Omega = \sum_n (f(\epsilon_n) - \mu) \epsilon_n = \sum_n f(\epsilon_n) \epsilon_n - \mu N_{el} \quad (16)$$

$$\rho(\mathbf{r}) = \sum_n f(\epsilon_n) \Psi_n^*(\mathbf{r}) \Psi_n(\mathbf{r}). \quad (17)$$

The function f is the the Fermi distribution

$$f(\epsilon) = \frac{1}{1 + \exp(\frac{\epsilon - \mu}{k_B T})}, \quad (18)$$

where k_B is Boltzmann's constant and T the temperature. If we talk about temperature in this article, we always mean the electronic temperature since we are not considering the motion of the ionic degrees of freedom which might be associated with a different ionic temperature. In the expressions (14), (15), (16), and (17), as well as in the remainder of the whole article, we will use the convention, that all the subscripts indexing eigenvalues

and eigenfunctions are combined orbital and spin indices, i.e. that we can put at most one electron in each orbital. This will eliminate bothering factors of 2. The usually relevant case of an unpolarized spin restricted system can always easily be obtained by cutting into half all sums over these indices and multiplying by 2.

In terms of the Hamiltonian H the density matrix is defined as the following matrix functional

$$F = f(H) . \quad (19)$$

Since F is a matrix function of H it has the same eigenfunctions Ψ_n as H

$$H\Psi_n = \epsilon_n \Psi_n \quad (20)$$

$$F\Psi_n = f(\epsilon_n) \Psi_n . \quad (21)$$

The density matrix can consequently be written as

$$F(\mathbf{r}, \mathbf{r}') = \sum_n f(\epsilon_n) \Psi_n^*(\mathbf{r}) \Psi_n(\mathbf{r}') , \quad (22)$$

where n runs over all the eigenstates of the Hamiltonian. From the functional form of the Fermi distribution it follows that the eigenvalues $f(\epsilon_n)$ are always in the interval [0:1]. At zero temperature the density matrix of an insulating system containing N_{el} electrons will have N_{el} eigenvalues of value one, all others being zero. Thus the density matrix does not have full rank, but only rank N_{el} . Hence we can write it as

$$F(\mathbf{r}, \mathbf{r}') = \sum_{n=occ} \Psi_n^*(\mathbf{r}) \Psi_n(\mathbf{r}') , \quad (23)$$

where n runs now only over the N_{el} occupied states. It is easy to see that $F(\mathbf{r}, \mathbf{r}')$ is a projection operator in this case

$$\int F(\mathbf{r}, \mathbf{r}'') F(\mathbf{r}'', \mathbf{r}') d\mathbf{r}'' = F(\mathbf{r}, \mathbf{r}') . \quad (24)$$

A new set of N_{el} eigenfunctions $\Psi_n^{new}(\mathbf{r})$ can be obtained by any unitary transformation of all the N_{el} degenerate eigenfunctions $\Psi_n(\mathbf{r})$ associated with eigenvalues one,

$$\Psi_n^{new}(\mathbf{r}) = \sum_{m=occ} U_{n,m} \Psi_m(\mathbf{r}) , \quad (25)$$

where U is a unitary N_{el} by N_{el} matrix. In the case of a crystalline periodic solids such a transformation can be used to generate the localized Wannier functions (Blount) from the extended eigenfunctions Ψ_n . We will refer to any set of orthogonal exponentially localized orbitals which can be used to represent the density matrix according to Equation (23) as Wannier functions. How to construct an optimally localized set of Wannier functions by the minimization of the total spread $\sum_n \langle r^2 \rangle_n - \langle \mathbf{r} \rangle_n^2$ in a crystalline periodic solid has recently been shown by Marzari and Vanderbilt (1997). It has been well known in the chemistry community (Chalvet 1976) that sets of maximally localized orbitals give excellent insight into the bonding properties of systems. In addition to the spread criterion used by Marzari *et al.* there are still other criteria in common use in the chemistry community. They are all in a certain sense arbitrary, but usually lead to the

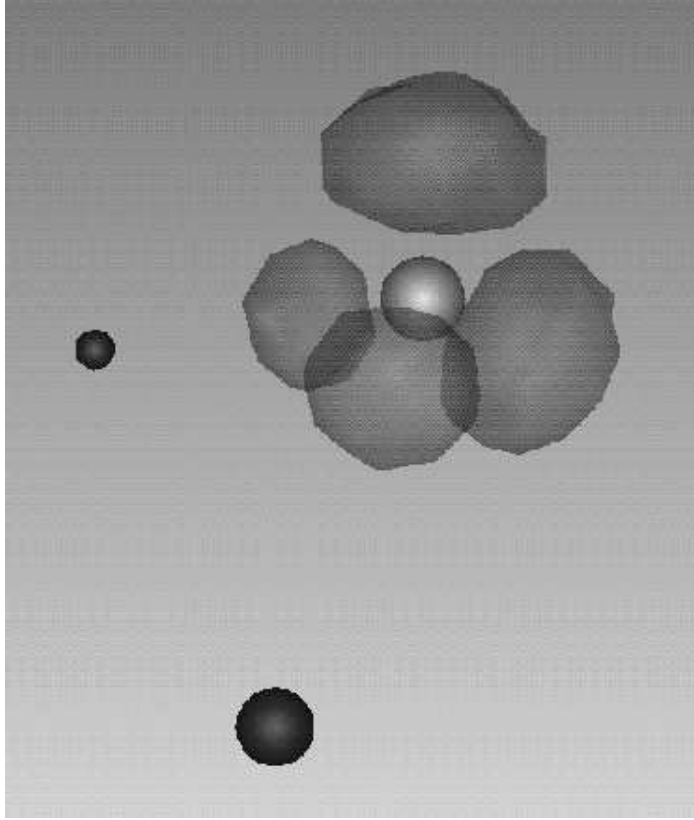


Figure 2: *A set of four Wannier orbitals (indicated by clouds) for the water molecule. The oxygen nucleus in the center is shown as a bright ball and the two hydrogen nuclei as nearly black balls. One sees two Wannier functions along the lines connecting the central oxygen with the two hydrogen atoms representing bonds as well as two lone electron pairs. The centers of the four Wannier functions form a nearly tetragonal structure.*

same interpretation of the bonding properties. Figure 2 shows the four Wannier functions for the water molecule.

The density matrix $F(\mathbf{r}, \mathbf{r}')$ is a diagonally dominant operator, whose off-diagonal elements decay with increasing distance from the diagonal. The exact decay behavior depends on the material. We will derive the decay properties within the theoretical framework of the description of periodic crystalline solids. For a periodic solid the density matrix is given by

$$\begin{aligned} F(\mathbf{r}, \mathbf{r}') &= \sum_n \frac{V}{(2\pi)^3} \int_{BZ} d\mathbf{k} f(\epsilon_n(\mathbf{k})) \Psi_{n,\mathbf{k}}^*(\mathbf{r}) \Psi_{n,\mathbf{k}}(\mathbf{r}') \\ &= \sum_n \frac{V}{(2\pi)^3} \int_{BZ} d\mathbf{k} f(\epsilon_n(\mathbf{k})) u_{n,\mathbf{k}}^*(\mathbf{r}) u_{n,\mathbf{k}}(\mathbf{r}') e^{i\mathbf{k}(\mathbf{r}' - \mathbf{r})}, \end{aligned} \quad (26)$$

where $\Psi_{n,\mathbf{k}}(\mathbf{r}) = u_{n,\mathbf{k}}(\mathbf{r}) e^{i\mathbf{k}(\mathbf{r})}$ are the Bloch functions associated with the wave vector \mathbf{k} and band index n . The integral is taken over the Brillouin zone (BZ) and V is the volume of the real space primitive cell.

The Wannier functions W_n of the n -th band in an insulating crystal are defined in the

usual way

$$W_n(\mathbf{r} - \mathbf{R}) = \frac{V}{(2\pi)^3} \int_{BZ} d\mathbf{k} e^{-i\mathbf{k}\mathbf{R}} \Psi_{n,\mathbf{k}}(\mathbf{r}) . \quad (27)$$

The Wannier functions are not uniquely defined. One can construct a different set of Bloch functions by multiplying them with a phase factor, $\Psi_{n,\mathbf{k}}(\mathbf{r}) \leftarrow e^{i\omega(\mathbf{k})} \Psi_{n,\mathbf{k}}(\mathbf{r})$, where $\omega(\mathbf{k})$ is an arbitrary function. This will obviously modify the Wannier functions. Further ambiguities arise in the case of degenerate bands (Blount). Because of these ambiguities in the construction of the Wannier functions it is advantageous to work with the density matrix where any phase factors cancel (Equation (26)) and where degeneracies do not cause any problems since one sums over all the occupied bands.

We will first discuss the decay properties of the density matrix in metallic systems. In this discussion we will assume that metals behave essentially like jellium and that exact results for jellium can be carried over to real metals.

The decay properties of the density matrix of a metallic system at zero temperature are well known (March). Because the integral in Equation (26) contains a discontinuity in the metallic case, the density matrix decays only algebraically with respect to the distance between \mathbf{r} and \mathbf{r}' . The decay is given by

$$F(\mathbf{r}, \mathbf{r}') \propto k_F \frac{\cos(k_F |\mathbf{r} - \mathbf{r}'|)}{|\mathbf{r} - \mathbf{r}'|^2} , \quad (28)$$

where the Fermi wave vector k_F is related to the valence electron density by $\frac{N_{el}}{V} = \frac{k_F^3}{3\pi^2}$ in a non-spin-polarized system.

Introducing a finite electronic temperature T in a metal leads to a drastic change in this decay behavior. Instead of an algebraic decay one has a much faster exponential decay. As shown independently by Goedecker (1998a) and Ismail-Beigi and Arias (1998), the decay at low temperatures is then given by

$$F(\mathbf{r}, \mathbf{r}') \propto k_F \frac{\cos(k_F |\mathbf{r} - \mathbf{r}'|)}{|\mathbf{r} - \mathbf{r}'|^2} \exp\left(-c \frac{k_B T}{k_F} |\mathbf{r} - \mathbf{r}'|\right) , \quad (29)$$

where c is a constant on the order of 1. We thus find oscillatory behavior with an exponentially damped amplitude. The decay rate depends linearly on temperature and the oscillatory part is described by the wave vector k_F . The related correlation function at finite temperature exhibits the same temperature dependence of the decay rate with respect to temperature (Landau and Lifshitz, 1980). In an insulator finite temperature plays no role as long as the thermal energy $k_B T$ is much smaller than the gap, which is usually fulfilled.

Let us next discuss the important case of an insulator with a band gap ϵ_{gap} at zero temperature. We will first present some numerical results, then we will put forward some arguments to explain the qualitative features of the density matrix and finally discuss in a more quantitative way the factors which determine the exact decay rate.

Numerical calculations of the density matrix or the related Wannier functions show an oscillatory behavior with a decaying amplitude. There is exactly one node per primitive cell and logarithmic plots of the amplitude clearly reveal an exponential decay. In the case of alkanes the decay of the density matrix calculated by the Hartree-Fock method has

been studied and plotted on a logarithmic scale by Maslem *et al.* (1997). Interestingly, the decay depends also on the basis set used. Small low quality basis sets lead to a larger band gap and consequently to a faster decay of the density matrix. In the case of silicon, treated by Density Functional theory, logarithmic plots revealing the exponential decay of the Wannier functions have also been done both for grid based basis sets (Goedecker unpublished) and atomic basis sets (Stephan 1998). Within the Tight Binding method the decay of the density matrix has also been studied numerically for crystalline and liquid carbon systems by Goedecker (1995) and for fullerenes by Itoh *et al.* (1996).

Let us now make plausible the exponential decay of the density matrix. The demonstration is based on the fact, that one can express the Fourier components $\epsilon_n(\mathbf{R})$ of the band energy $\epsilon_n(\mathbf{k})$ through the Wannier functions $W_n(\mathbf{r})$

$$\epsilon_n(\mathbf{R}) = \frac{V}{(2\pi)^3} \int_{BZ} \epsilon_n(\mathbf{k}) e^{-i\mathbf{k}\mathbf{R}} d\mathbf{k} = \frac{(2\pi)^3}{V} \int_{space} W_n^*(\mathbf{r}') H W_n(\mathbf{r}' - \mathbf{R}) d\mathbf{r}', \quad (30)$$

where \mathbf{R} is a Bravais lattice vector. Now it is known, that the band energy $\epsilon_n(\mathbf{k})$ is an analytic function (Blount). This is actually not surprising. The first and second derivatives of the band-structure have physical meaning since they are related to the electron velocity and effective mass. So it is to be expected that higher derivatives exist as well. Since the Fourier transform of an analytic function decays faster than algebraically (See Appendix) there exists a decay constant γ and a normalization constant C such that

$$Ce^{-\gamma R} \geq \epsilon_n(\mathbf{R}) = \frac{1}{V} \int_{space} W_n^*(\mathbf{r}') H W_n(\mathbf{r}' - \mathbf{R}) d\mathbf{r}' \quad (31)$$

It is reasonable to expect that $H W_n(\mathbf{r})$ will behave similarly as $W_n(\mathbf{r})$. In particular we expect $W_n(\mathbf{r})$ to be small whenever $H W_n(\mathbf{r})$ is small. So we will just drop H in Equation (31). In addition we will define this modified integral not only for lattice vectors \mathbf{R} but for arbitrary vectors \mathbf{r} to obtain.

$$Ce^{-\gamma r} \geq \frac{1}{V} \int_{space} W_n^*(\mathbf{r}') W_n(\mathbf{r}' - \mathbf{r}) d\mathbf{r}' \quad (32)$$

If Equation (32) holds, then one can use the mean value theorem to show that

$$\begin{aligned} Ce^{-\gamma r} &\geq \frac{1}{V} \int_{space} W_n^*(\mathbf{r}') W_n(\mathbf{r}' - \mathbf{r}) d\mathbf{r}' \\ &= \frac{1}{V} \sum_{\mathbf{R}'} \int_{cell} W_n^*(\mathbf{r}' - \mathbf{R}') W_n(\mathbf{r}' - \mathbf{R}' - \mathbf{r}) d\mathbf{r}' \\ &= \sum_{\mathbf{R}'} W_n^*(\mathbf{s}(\mathbf{r}) - \mathbf{R}') W_n(\mathbf{s}(\mathbf{r}) - \mathbf{R}' - \mathbf{r}) d\mathbf{r}' \\ &= F(\mathbf{s}(\mathbf{r}), \mathbf{s}(\mathbf{r}) - \mathbf{r}) \end{aligned} \quad (33)$$

where the mean value $\mathbf{s}(\mathbf{r})$ is a vector within the primitive cell. Assuming that the density matrix has the same order of magnitude within each cell one can neglect the dependence of \mathbf{s} on \mathbf{r} to obtain the final result

$$Ce^{-\gamma r} \geq F(\mathbf{s}, \mathbf{s} - \mathbf{r}) \quad (34)$$

The numerically observed nodal structure of the density matrix can be motivated in a very similar way. Because of the orthogonality of the Wannier functions we have

$$0 = \int_{space} W_n^*(\mathbf{r}') W_n(\mathbf{r}' - \mathbf{R}) d\mathbf{r}' \quad (35)$$

for any non-zero lattice vector \mathbf{R} . Doing the same sequence of transformation as in Equation (33) one obtains

$$0 = F(\mathbf{s}(\mathbf{R}), \mathbf{s}(\mathbf{R}) - \mathbf{R}) \quad (36)$$

So there has to be one node in each cell. The numerically calculated nodal structure for a 1-dimensional model insulator is shown in Figure 3.

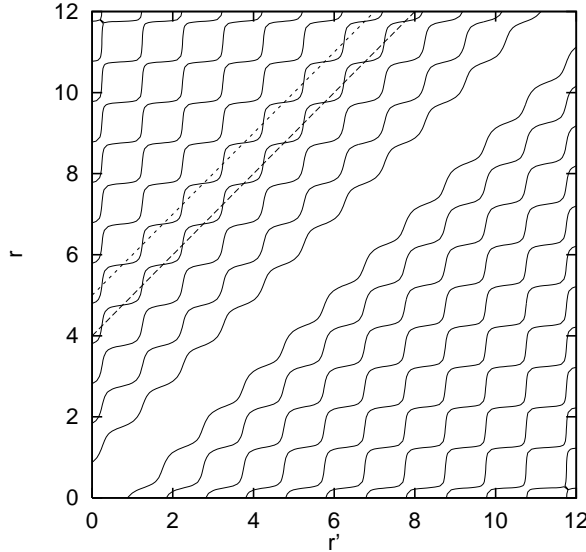


Figure 3: *The nodal structure of the density matrix for a 1-dimensional model insulator with a bandwidth of 4 a.u. and a band gap of 2 a.u.. The length of the primitive cell is 1. The nodes predicted by Equation (36) are at the intersections with diagonal lines, two of which are shown by the dashed lines.*

The next step is to examine in a more quantitative way which factors determine the rate of this exponential decay for an insulator with a band gap ϵ_{gap} at zero temperature.

Cloizeaux (1964) proved the exponential decay behavior of the zero temperature density matrix, which is a projection operator. Considering the extension of the band energy $\epsilon_n(\mathbf{k})$ into the complex \mathbf{k} plane he found that the minimal distance of the branch points of $\epsilon_n(\mathbf{k})$ from the real axis determines the decay behavior. For the Wannier functions, which are closely related to the density matrix by Equation (23), Kohn (1959) proved the same decay behavior in the case of a one-dimensional model crystal. In a later publication Kohn (1993) claims that this distance to the real \mathbf{k} axis should be related to the square root of the gap. Even though he did not present a derivation of this result, it was widely accepted to be generally valid. Ismail-Beigi and Arias (1998) have however shown that Kohn's claim is not generally valid. They demonstrated that in the Tight Binding limit the square root behavior can be found under certain circumstances, but that different

behaviors can be found as well. In the weak binding limit, where the band-structure can be obtained by perturbation theory from the band structure of the free electron gas, they showed that the dependence is actually linear.

$$F(\mathbf{r}, \mathbf{r}') \propto \exp(-\gamma|\mathbf{r} - \mathbf{r}'|) \quad \text{where } \gamma = c \epsilon_{gap} a \quad (37)$$

The lattice constant is denoted by a , and c is an unknown constant of the order of 1.

The dependence of the decay rate on the size of the band gap is a rather surprising relation. After all it follows from Equation (26) that only the properties of the occupied bands enter into the calculation of the density matrix, whereas the size of the gap is not directly related to the occupied states. In the following we will give an intuitive explanation of the factors determining the decay rate. This explanation will again be based on Equation (30) relating the bandstructure to the decay properties of the density matrix. As is known from complex analysis, the distance of the singularities from the real axis is comparable to the length over which one has very strong variations along the real axis of a complex function. Now, the long range decay properties of a Fourier transform are exactly determined by the length Δk of such a region of strongest variation (See Appendix). One thus regains Cloizeaux's result that the decay rate is proportional to the distance of singularities from the real axis. Let us now explain the behavior found in the weak binding limit by Ismail-Beigi and Arias. In the weak binding limit the effective mass establishes the connection between the gap and the important features of the occupied bands. The effective mass for the n -th band at the point \mathbf{k}_0 is defined as (Kittel 1963)

$$\frac{1}{m} = 1 + \frac{2}{3} \sum_{m \neq n} \frac{|\int \Psi_{n, \mathbf{k}_0}^*(\mathbf{r}) \nabla \Psi_{m, \mathbf{k}_0}(\mathbf{r}) d\mathbf{r}|^2}{\epsilon_n(\mathbf{k}_0) - \epsilon_m(\mathbf{k}_0)} \quad (38)$$

Since we are only interested in order of magnitudes, we have here averaged over the diagonal elements of the effective mass tensor in order to obtain a effective mass which is a scalar quantity. In the case of the weak binding limit, a gap will open up at the boundaries of the Brioullin zone and this gap will be small. The effective mass is therefore small and proportional to $a^2 \epsilon_{gap}$, where we have assumed that the dipole matrix elements $\int \Psi_{n, \mathbf{k}_0}^*(\mathbf{r}) \nabla \Psi_{i, \mathbf{k}_0}(\mathbf{r}) d\mathbf{r}$ are on the order of $\frac{1}{a}$. The band-structure near the boundaries of the Brioullin zone is then given by

$$\frac{1}{2m} (\Delta k)^2 \propto \frac{1}{a^2 \epsilon_{gap}} (\Delta k)^2 \quad (39)$$

where Δk is the distance from the boundary, neglecting directional effects. Since the effective mass is small, the curvature of the band-structure is large in this region. Hence this region is just the region with the strongest variation. As is well known (Ashcroft and Mermin 1976), the perturbation theory arguments leading to Equation (39) are valid within an energy range of the order of ϵ_{gap} . It then follows from Equation (39) that the corresponding range of Δk is $\epsilon_{gap} a$, confirming the linear decay of the density matrix with respect to the size of the gap, i.e. $\gamma = c \epsilon_{gap} a$.

Let us next show how a square root like behavior $\gamma = c \sqrt{\epsilon_{gap}}$ can arise for real crystals with a big gap. In this case the effective mass is of the order of one at all stationary points \mathbf{k}_0 in the Brioullin zone. Assuming that it is then of the order of one over the

whole Brioullin zone, the region of largest variation is just the Brillouin zone itself. The decay constant is therefore simply related to the lattice constant a .

$$\gamma = c \frac{1}{a} \quad (40)$$

In order to get the square root dependence of the decay constant γ , one has to assume that

$$\epsilon_{gap} = C_{gap} \frac{1}{a^2} \quad (41)$$

where C_{gap} is a constant which is not or only weakly dependent on the material. Such a behavior has indeed been observed for certain classes of materials, where the tight binding limit is the most appropriate one, such as ionic crystals (Harrison 1980), but with a non-negligible variation of C_{gap} across different materials. A square root behavior of γ can therefore be expected if one varies the lattice constant for a certain material, but the decay constants for different materials that happen to have the same gap are not necessarily comparable.

In practice the distinction between the Tight Binding and weak binding case may not always be clear. Unless the region of strongest variation is really a very small fraction of the whole Brioullin zone, all the prefactors which were neglected in these considerations might be important enough to blur out differences. The importance of these prefactors can also be seen from the fairly strong directional dependence of the decay rate. Ismail-Beigi and Arias (1998) found such a strong directional dependence in numerical tests to confirm the linear dependence of the decay constant on the size of the gap (Figure 4). Stephan *et al.* (1998) found the same behavior during Tight Binding studies of carbon. So a statement in an old paper by Kohn (1964), namely that the decay length of the Wannier functions is of the order of the interatomic spacing, is for practical purposes probably in many cases the best available characterization of localization.

As a numerical illustration of this surprising result, that only a small part of the Brillouin zone where one has the strongest variation determines the decay behavior of the Wannier functions, we compared the decay behavior of carbon in the diamond structure with "syntheticum" in the same structure. The artificial element "syntheticum" was computer generated within the Tight Binding context in such a way that its top part of the conduction band as well as the gap is nearly identical to real carbon, whereas the lower part of the valence band is drastically different as shown in Figure 5. More precisely, Carbon was characterized by the parameters of Goodwin (1991) and to obtain syntheticum ϵ_s was modified from -5.16331 to -1.16331 and $V_{ss\sigma}$ was modified from -4.43338 to -2.43338.

Figure 6 shows the decay behavior of the density matrix. As one can see the decay behavior is very similar in both cases. We note that not only the gap is similar but also the effective mass since the density of states at the top of the valence band has the same behavior in both materials.

All the above arguments apply to simple and mainly periodic materials. Advanced electronic structure calculations however frequently study materials which are not in this class. The localization properties of such materials have not yet been studied systematically and so there is some incertitude about which orbitals are localized and to what extent (Kohn 1995). If the localization properties are unknown one should better not impose any localization constraints. In this case some of the discussed O(N) techniques still

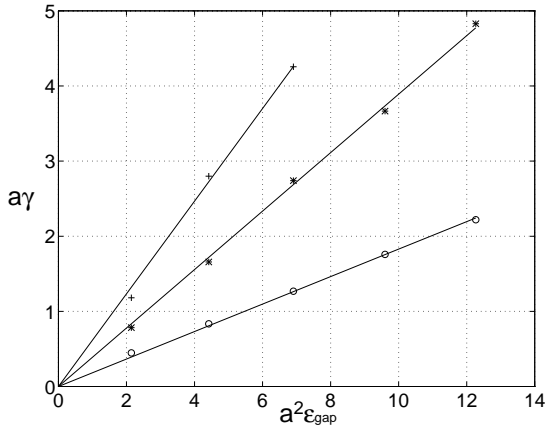


Figure 4: *The dependence of the decay constant γ on the gap. Plotted are the two dimensionless quantities $a\gamma$ versus $a^2\epsilon_{\text{gap}}$. The variation of the gap was obtained for a three-dimensional cubic model crystal by varying the strength of the potential. Circles refer to the [100], stars to the [110] and pluses to the [111] direction. This figure is reproduced with kind permission of the authors from Ismail-Beigi and Arias (1998)*

give a quadratic scaling, which also allows us to gain computational efficiency compared to the traditional cubically scaling algorithms.

3 Basic strategies for $O(N)$ scaling

Most $O(N)$ algorithms are built around the density matrix or its representation in terms of Wannier functions and take advantage of its decay properties. To obtain linear scaling one has to cut off the exponentially decaying quantities when they are small enough. This introduces the concept of a localization region. Only inside this localization region the quantity is calculated, outside it is assumed to vanish. For simplicity the localization region is usually taken to be a sphere, even though the optimal shape might be different (Stephan 1998). In the Tight Binding context the boundary of the localization region can either be defined by a geometric distance criterion or in terms of the number of "hops", i.e. the number of steps one has to do along bonds connecting neighboring atoms to reach this boundary (Voter *et al.*, 1996). Different localization regions generally have significant overlaps. The localization regions thus do not form a partition of the computational volume and one atom in general belongs to several localization regions.

In a numerical calculation the density operator $F(r, r')$ is discretized with respect to a basis. The basis set has to be chosen such that the matrix elements $F_{i,j}$ reflect the decay properties of the operator $F(r, r')$. This will obviously only be the case if the basis set consists of localized functions, such as atom centered Gaussian type basis functions. Sets of orthonormal basis functions usually facilitate the calculations. Unfortunately all currently used localized basis sets are non-orthogonal. In the context of the orthogonal Tight Binding scheme (Goringe *et al.*, 1997a, Majewski and Vogl 1986) one just assumes the existence of an basis set which is both atom centered and orthogonal. Since only

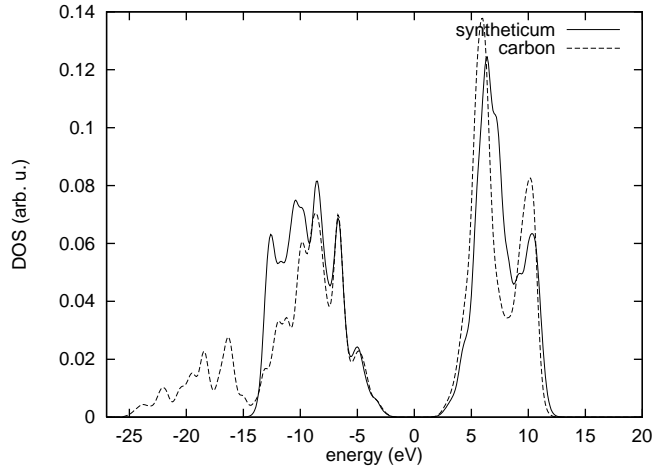


Figure 5: *Comparison of the density of states of carbon and syntheticum. As one sees both have roughly the same gap. The lower part of the valence band is however drastically different. The valance band of syntheticum is roughly only half as wide as the one of carbon*

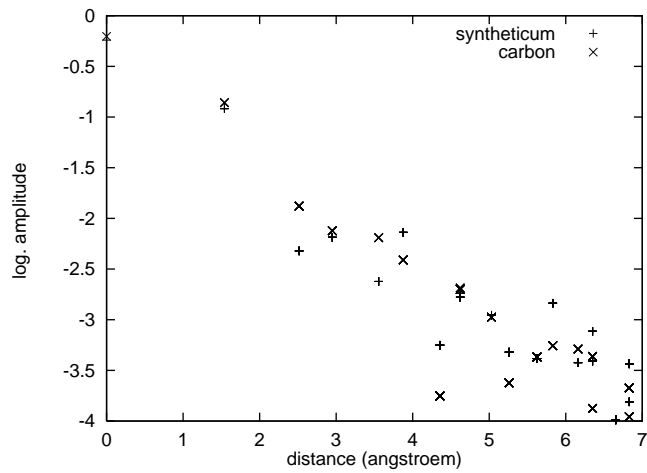


Figure 6: *Comparison of the decay behavior of the density matrices for carbon and syntheticum. They are both very similar. The moderate scattering comes from the fact that the density matrix does not decay equally fast in all directions*

the parameterized Hamiltonian matrix elements enter in the calculation, there is no need to explicitly ever construct such a basis set. In the following sections, we will follow this practice and assume in all relevant parts that we are dealing with such a localized orthogonal basis set. The non-orthogonal case will be discussed in section 7. Whenever we refer from now on to a localization region, we actually mean the subset of all basis functions which are contained within this spatial localization region.

Obviously the size of the localization region needed to obtain a certain accuracy depends on the decay properties of the density matrix as well as on the selected accuracy threshold. It also depends on the quantity one wants to study. Generally, the total energy as well as derived quantities such as the geometric equilibrium configurations are surprisingly insensitive to finite localization regions, because these quantities are not strongly influenced by the exponentially small tails which are cut off by the introduction of a localization region. This insensitivity also holds true, even though to a much lesser extent, for metals. As we have seen above the introduction of a finite temperature leads to an exponential decay of the density matrix which in turn justifies truncation. In a metal, the difference between the finite and the zero temperature total energy ΔE is proportional to the square of the temperature, $\Delta E \propto T^2$, (Ashcroft and Mermin 1976) and thus rather small. There are however quantities which are very sensitive to finite localization regions. In the modern theory of polarization in solids (King-Smith and Vanderbilt 1989), the polarization can be expressed in terms of the centers of the Wannier functions $\int W(\mathbf{r})\mathbf{r}W(\mathbf{r})d\mathbf{r}$. Using this formula (Fernandez *et al.*, 1997) one has a strong influence of the tails of the Wannier functions because they get strongly weighted by the factor of \mathbf{r} in the integral. Since the tails are much more influenced by the boundary of the localization region than the central part, this quantity is more sensitive to the size of the localization region.

There are even quantities which are not at all directly accessible by a solution which is given in terms of density matrices or Wannier functions. The Fermi surface in a metal which can be calculated via the eigenvalues of the band structure $\epsilon_n(\mathbf{k})$ is such an example.

It is also clear that one can gain significant computational efficiency only if the size of the system is larger than the size of the localization region. When this criterion is fulfilled depends not only on the decay properties of the density matrix of the system but also on its dimensionality. In the case of a linear chain molecule with a large band gap, it might be enough to have a localization region containing just two neighboring atoms on each side. So the localization region would just contain 5 atoms and for systems larger than 5 atoms one might potentially gain computational efficiency by using an $O(N)$ method. If one has a 3 dimensional system with a comparable gap, then a spherical localization region extending out to the second neighbors would contain some 60 atoms and the crossover point would already be much larger. For a system with a small gap such as silicon or for metallic systems the crossover point is even larger.

There are essentially six basic approaches to achieve linear scaling.

- The Fermi Operator Expansion (FOE) is based on Equation (19). In this approach one finds a computable functional form of F as a function of H to build up the density matrix. Two possible representations based on a Chebychev expansion and a rational expansion will be discussed.

- The Fermi Operator Projection (FOP) is closely related to the FOE method. The computable form of F is however not used to construct the entire density matrix but to find the space spanned by the occupied states, i.e. the space corresponding to the eigenfunctions associated with the unit eigenvalues of the Density matrix at zero temperature. These eigenfunctions can be considered as Wannier functions in the generalized sense defined before.
- In the Divide and Conquer (DC) method for the density matrix the relevant parts of the density matrix are patched together from pieces that were calculated for smaller subsystems.
- In the Density Matrix Minimization (DMM) approach, one finds the density matrix by a minimization of an energy expression based on the density matrix.
- In the Orbital Minimization approach (OM), one finds a set of Wannier functions by minimization of an energy expression.
- The Optimal Basis Density Matrix Minimization scheme (OBDMM) contains aspects of both the OM and DMM methods. In addition to finding a density matrix with respect to the basis, one also finds an optimal basis by additional minimization steps. The number of basis functions has to be at least equal to the number of electrons in the system, but can be bigger as well.

A major difference between these methods is whether they calculate the full density matrix or only its representation in terms of Wannier functions. The later approach applies only to insulators while the former is in also applicable to systems with fractional occupation numbers (i.e. $f(\epsilon_n)$ is not either 1 or 0) such as metals or systems at finite electronic temperature.

In the following each of these six approaches will be presented in detail.

3.1 The Fermi Operator Expansion

The FOE (Goedecker and Colombo 1994, Goedecker and Teter 1995) is the most straightforward approach for the calculation of the density matrix. The basic idea in this approach is to find a representation of the matrix function (19) which can be evaluated on a computer. Several such representations are possible. We will discuss a Chebychev and a rational representation.

3.1.1 The Chebychev Fermi Operator Expansion

One of the most basic operations a computer can do are matrix times vector multiplications. The simplest representation of the density matrix would therefore be a polynomial representation

$$F \approx p(H) = c_0 I + c_1 H + c_2 H^2 + \dots + c_{n_{pl}} H^{n_{pl}}.$$

where I is the identity matrix. Unfortunately polynomials of high degree become numerically unstable. This instability can however be avoided by introducing a Chebychev

polynomial representation, which is a widely used numerical method (Press *et al.*, 1986)

$$p(H) = \frac{c_0}{2} I + \sum_{j=1}^{n_{pl}} c_j T_j(H) . \quad (42)$$

Since the Chebychev polynomials are defined only within the interval [-1:1], we will assume in the following that the eigenvalue spectrum of H falls within this interval. This can always be easily achieved by scaling and shifting of the original Hamiltonian. The Chebyshev matrix polynomials $T_j(H)$ satisfy the recursion relations

$$T_0(H) = I \quad (43)$$

$$T_1(H) = H \quad (44)$$

$$T_{j+1}(H) = 2H T_j(H) - T_{j-1}(H) . \quad (45)$$

The expansion coefficients of the Chebychev expansion can easily be determined. The eigenfunction representation (Equation (21)) of F is,

$$\langle \Psi_n | F | \Psi_m \rangle = f(\epsilon_n) \delta_{n,m} . \quad (46)$$

Evaluating the polynomial expansion in the same eigenfunction representation we obtain

$$\langle \Psi_n | p(H) | \Psi_m \rangle = p(\epsilon_n) \delta_{n,m} , \quad (47)$$

where

$$p(\epsilon) = \frac{c_0}{2} + \sum_{j=1}^{n_{pl}} c_j T_j(\epsilon) . \quad (48)$$

Comparing Equation (46) and Equation (47) we see that the polynomial $p(\epsilon)$ has to approximate the Fermi distribution in the energy interval [-1:1] where the scaled and shifted Hamiltonian has its eigenvalues. How to find the Chebychev expansion coefficients for a scalar function is described in standard textbooks on numerical analysis (Press *et al.*, 1986). Actually it is not necessary to take the exact Fermi distribution. In practically all situations one is interested in the limit of zero temperature. Hence any function which approaches a step functions in the limit of zero temperature can be used. In the case of simulations of insulators for instance it is advantageous to take the function $f(\epsilon) = \frac{1}{2}(1 - \text{erf}(\frac{\epsilon - \mu}{\Delta\epsilon}))$ shown in Figure 7 since it decays faster to 0 respectively 1 away from the chemical potential. The term Fermi distribution will in the following always be used in this broader sense. The energy resolution $\Delta\epsilon$ is chosen to be a certain fraction of the size of the gap (Goedecker and Teter 1995). In the case of metals, $\Delta\epsilon$ is chosen by considerations of numerical convenience. Large values of $\Delta\epsilon$ will give lower accuracy results. However as pointed out before, the convergence of the total energy with respect to $\Delta\epsilon$ is quadratic and so highly accurate total energies can be obtained with rather high values of $\Delta\epsilon$ (Goedecker and Teter 1995). Small values of $\Delta\epsilon$ make the calculation numerically expensive. The detailed scaling behavior of the numerical effort in the limit of vanishing gaps is analyzed in section 4, where it is found that actually the increase in the size of the localization region is the limiting factor in all methods.

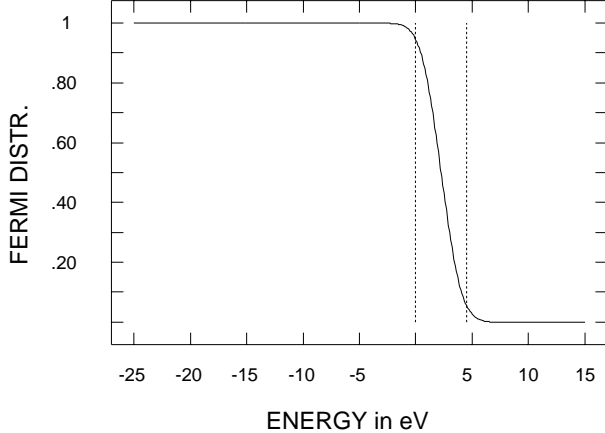


Figure 7: *The Fermi distribution as obtained by a Chebychev fit of degree 40 in the case of a diamond structure. The bandgap is in between the two vertical lines.*

Even if one wants to study electronic properties in the limit of zero electronic temperature it is important that one nevertheless uses a finite temperature Fermi distribution for the Chebychev fit. Using the zero temperature step function introduces so-called Gibbs oscillations in the fit and spoils the Chebychev fit over the whole interval.

How to eliminate these Gibbs oscillations in the zero temperature case by the so called kernel polynomial method (Voter *et al.*, 1996, Silver *et al.*, 1996) can be used as a starting point for an alternative derivation of the FOE method. The basic idea is to expand a delta function as a polynomial using damping factors to suppress large oscillations. This representation of an approximate delta function can then be integrated to obtain a smooth representation of the Fermi distribution. Used this way the kernel polynomial method is thus just another way to derive the expansion coefficients for the Chebychev expansion (Kress *et al.*, 1998). In addition the kernel polynomial method can also be used to smear out the density of states rather than the zero temperature Fermi distribution resulting in a method with practically identical computational requirements but some slightly different properties. One useful property is that the smeared density of states energy is an approximate lower bound to the energy, whereas the smeared Fermi energy is an approximate upper bound (Voter *et al.*, 1996).

Coming back to the original motivation for a polynomial representation, let us now show how the density matrix can be constructed using only matrix times vector multiplications. Let us denote by t_l^j the l -th column of the Chebychev matrix T_j . Now each column of these Chebychev matrices satisfies the same recursion relations

$$\begin{aligned}
 |t_l^0\rangle &= |e_l\rangle \\
 |t_l^1\rangle &= H|e_l\rangle \\
 |t_l^{j+1}\rangle &= 2H|t_l^j\rangle - |t_l^{j-1}\rangle .
 \end{aligned} \tag{49}$$

where e_l is a unit vector that has zeroes everywhere except at the l -th entry. So Equation (49) demonstrates that we indeed need only matrix vector multiplications. Once we have generated the l -th columns of all the Chebychev matrices, we can obtain the l -th

column f_l of the density matrix just by forming linear combinations

$$|f_l\rangle = \frac{c_0}{2}|t_l^0\rangle + \sum_{j=1}^{n_{pl}} c_j|t_l^j\rangle. \quad (50)$$

As we have described the method so far it has a quadratic scaling instead of the linear scaling we finally want to achieve. If we have M_b basis functions, the density matrix is a $M_b \times M_b$ matrix and we have to calculate M_b full columns. For the calculation of each column, we have to do n_{pl} matrix times vector multiplications, each of which costs $M_b n_H$ operations assuming the matrix H is a sparse matrix with n_H off-diagonal elements per row/column. So the total computational cost is $M_b^2 n_{pl} n_H$. The degree of the polynomial n_{pl} and the width n_H of the Hamiltonian are independent of the size of the system, whereas M_b is proportional to the number of atoms in the system. The overall scaling with respect to the number of atoms is therefore quadratic.

In order to do the correct shifting and scaling of the original Hamilton to map its eigenvalue spectrum on the interval [-1:1] we have to know its lowest and highest eigenvalues ϵ_{min} and ϵ_{max} . In addition we have to know the chemical potential μ . There are auxiliary matrix functions of H that can help us to determine these quantities. These functions of H can be build up in the same way as the density matrix. Since the recursive build up of the Chebychev matrices is the most costly part, the additional cost for evaluating other functions is negligible. To determine whether we have a vanishing density of states beyond an energy ϵ_{up} we can for instance construct a Chebychev fit $p_{up}(\epsilon)$ to a function which is zero (to within a certain tolerance) for energies below ϵ_{up} , but blows up for energies larger than ϵ_{up} . If $Tr[p_{up}(H)]$ does not vanish we have a non-vanishing density of states beyond ϵ_{up} . A similar procedure can be applied to determine a lower bound for the density of states. The determination of the chemical potential in an insulator can be done along the same lines as well (Bates and Scuseria 1998). Without any significant extra cost one can build up several Fermi distributions with different chemical potentials until one finds the correct chemical potential leading to charge neutrality. In a metallic system the search for the chemical potential can be accelerated since it is possible to predict with high accuracy how the number of electrons changes in response to a change in the chemical potential. From Equation (13) it follows

$$\frac{\partial N_{el}}{\partial \mu} = -Tr[p'(H)], \quad (51)$$

where p' is the derivative of the Chebychev polynomial p that approximates the Fermi distribution. The Chebychev expansion coefficients of p' can be calculated from the coefficients for p (Press *et al.*, 1986). Using the finite difference approximation of Equation (51),

$$\Delta\mu = \frac{\Delta N_{el}}{Tr[p'(H)]}, \quad (52)$$

it is possible to find the correction $\Delta\mu$ to the chemical potential which will nearly exactly eliminate an excess of ΔN_{el} electrons due to an incorrect initial chemical potential. The correct chemical potential in a metallic system can thus be found with very high accuracy with a few iterations.

The desired linear scaling can be obtained by introducing a localization region for each column, outside of which the elements are negligibly small. For the k -th column, this localization region will be centered on the k -th basis function. If we use atom centered basis functions, then the localization region will consequently be centered on the atom to which this k -th basis function belongs. We have then to calculate only that part of each column which corresponds to this localization region. This means that we can use a truncated Hamiltonian $H(k)$ which retains only the matrix elements corresponding to the basis functions contained within the localization region k . Denoting the number of basis functions in this region by M_{loc} (which might actually depend on the localization region k being considered), the overall computational cost is then $M_b M_{loc} n_{pl} n_H$ and thus scales linearly. Let us stress, that the size of the localization region is independent of the degree of the polynomial. If one uses for instance a polynomial of degree $n_{pl} = 50$, the recursion in Equation (49) will extend over the 50 nearest neighbor shells without localization constraint for a Hamiltonian coupling only nearest neighbors. The localization region however is typically much smaller comprising just a few nearest neighbor shells. Imposing a localization region introduces some subtleties. For instance the eigenvalues of the truncated density matrix are not anymore exactly given by $p(\epsilon_n)$ and F is not any more strictly symmetric. More importantly, strictly speaking we can no longer use the Trace notation, since we use different local Hamiltonians $H(k)$ to build up the different columns of the density matrix. The band-structure energy E_{BS} has now to be written as

$$E_{BS} = \sum_k \sum_j [p(H(k))]_{k,j} [H(k)]_{j,k} . \quad (53)$$

Another important quantity are the forces. The force acting on the α -th atom at position R_α is obtained by differentiating the total energy with respect to these positions. The total energy consists of the band structure part and possibly other contributions. We will only discuss the non-trivial part of the force arising from the differentiation of the band structure energy E_{BS} . For simplicity let us assume that we have a simple polynomial expansion and not a Chebychev expansion. Let us also assume that we calculate the full density matrix, i.e. that we do not truncate H by introducing a localization region. We then obtain

$$\frac{dE_{BS}}{dR_\alpha} = \frac{d}{dR_\alpha} \text{Tr} \left[H \sum_\nu c_\nu H^\nu \right] = \sum_\nu c_\nu \text{Tr} \left[\frac{\partial H^{\nu+1}}{\partial R_\alpha} \right] . \quad (54)$$

Let us consider for instance the term for which $\nu = 2$

$$\frac{d\text{Tr}[H^3]}{dR_\alpha} = \text{Tr} \left[HH \frac{\partial H}{\partial R_\alpha} \right] + \text{Tr} \left[H \frac{\partial H}{\partial R_\alpha} H \right] + \text{Tr} \left[\frac{\partial H}{\partial R_\alpha} HH \right] = 3 \text{Tr} \left[HH \frac{\partial H}{\partial R_\alpha} \right] , \quad (55)$$

where we used that $\text{Tr}[AB] = \text{Tr}[BA]$. The final result for the force, which also holds in the case of a Chebychev expansion, is thus

$$\frac{dE_{BS}}{dR_\alpha} = \text{Tr} \left[(p(H) + Hp'(H)) \frac{\partial H}{\partial R_\alpha} \right] . \quad (56)$$

In the case of an insulator, the second term in the brackets $Hp'(H)$ is very small compared to the first term $p(H)$ at small but finite temperatures and it vanishes in the limit of zero

temperature. The reason for this is that the eigenvalues of the matrix $p'(H)$ are $p'(\epsilon_n)$. Since at zero temperature $p'(\epsilon)$ is nonzero only at the chemical potential which is in the middle of the gap, all eigenvalues are zero and the matrix is identically zero. Nevertheless it is recommendable to retain this term in numerical calculations because it leads to forces consistent with the total energy.

In the case where we calculate only part of the density matrix, i.e. where we have a truncated Hamiltonian $H(k)$ going with the energy expression (53) we cannot use the properties of the trace to simplify the force expression as we did in Equation (55). The equation corresponding to Equation (55) therefore reads

$$\begin{aligned} \sum_{k,j_1,j_2,k} & [H(k)]_{k,j_1} [H(k)]_{j_1,j_2} \left(\frac{\partial H(k)}{\partial R_\alpha} \right)_{j_2,k} + \\ & [H(k)]_{k,j_1} \left(\frac{\partial H(k)}{\partial R_\alpha} \right)_{j_1,j_2} [H(k)]_{j_2,k} + \\ & \left(\frac{\partial H(k)}{\partial R_\alpha} \right)_{k,j_1} [H(k)]_{j_1,j_2} [H(k)]_{j_2,k}. \end{aligned} \quad (57)$$

Similar results hold for all the other terms with different values of ν . In the case of a Chebychev expansion the situation is completely analogous, just the formulas are more complicated. The force formula has been worked out in this case by Voter *et al.* (1996) and is given by

$$\frac{dT_j(H)}{dR_\alpha} = \frac{dT_{j-2}(H)}{dR_\alpha} + \sum_{i=0}^{j-1} (1+k_i)(1+k_{j-1-i}) T_i(H) \frac{\partial H}{\partial R_\alpha} T_{j-1-i}(H), \quad (58)$$

where $k_j = 0$ if $j \leq 0$ and $k_j = 1$ otherwise. In the typical Tight Binding context $\frac{\partial H}{\partial R_\alpha}$ is a very sparse matrix. If it contains n_D non-zero elements, we need of the order of $n_{pl}^2 n_D M_b$ operations to evaluate all the forces according to Equation (58). The error incurred by using the approximate formula (56) based on the trace is usually negligible if the localization region is large enough. Since the approximate formula can be evaluated with order $n_{pl} n_D M_b$ operations, it might actually be preferable to do so. In a molecular dynamics simulation, the largest deviations in the conservation of the total energy come from events where atoms enter or leave localization regions and this kind of error is not taken into account by either force formula.

All the above force formulas were derived for the case where we have a constant chemical potential and where the polynomial representing the Fermi distribution does thus not change. Frequently one wants however to do simulations for a fixed number of electrons rather than for a fixed chemical potential. In this case one has to readjust the chemical potential for each new atomic configuration. The chemical potential is thus a function of all the atomic positions $\mu = \mu(R_\alpha)$, but the explicit functional form of this dependence is not known. The force formula can however also be adapted to this case (B. Roberts and P. Clancy 1998). Ignoring the above warnings and using again trace notation for simplicity we have

$$E_{BS} = \text{Tr}[H p(H - \mu I)] \quad (59)$$

$$N_{el} = \text{Tr}[p(H - \mu I)] \quad (60)$$

and consequently

$$\frac{dE_{BS}}{dR_\alpha} = Tr \left[(H p' + p) \frac{\partial H}{\partial R_\alpha} \right] - Tr[(H p')] \frac{\partial \mu}{\partial R_\alpha} \quad (61)$$

$$\frac{dN_{el}}{dR_\alpha} = Tr \left[p' \frac{\partial H}{\partial R_\alpha} \right] - Tr[p'] \frac{\partial \mu}{\partial R_\alpha}. \quad (62)$$

Since $\frac{dN_{el}}{dR_\alpha}$ has to be equal to zero, we can solve Equation (62) for $\frac{\partial \mu}{\partial R_\alpha}$ and insert it into equation (61) to obtain the force under the constraint of a constant number of electrons.

Let us finally derive a force formula for the case where a local charge neutrality condition is enforced (Kress *et al.*, 1998). The motivation for this approach is that in non-self-consistent Tight Binding calculations one frequently finds an unphysically large transfer of charge between atoms. In a self-consistent calculation the electrostatic potential, built up by a charge transfer, is counteracting a further charge flow and thus limits charge transfer to reasonably small values. Some Tight Binding schemes (Horsfield *et al.*, 1996a) enforce a so-called local charge neutrality condition requiring that the total charge associated with an atom in a molecule or solid be equal to the charge of the isolated atom. This is done by determining a potential offset u_α for each atom α in the system which will ensure this neutrality. The total Hamiltonian H of the system is then given by $H_0 + U$ where H_0 is the Hamiltonian without any potential bias and U a diagonal matrix containing the atomic potential offsets u_α . The band structure energy is given by

$$E_{BS} = Tr[(H_0 + U) p(H_0 + U)] - \sum_\alpha Q_\alpha u_\alpha, \quad (63)$$

where the term containing the atomic valence charges Q_α has been subtracted to make the expression invariant under the application of a uniform potential bias to all atoms in the system. Expressed in terms of the density matrix the local charge neutrality condition becomes

$$\sum_l p(H)_{\alpha,l;\alpha,l} = Q_\alpha. \quad (64)$$

In Equation (64) we have labeled the basis functions by a composite index where α indicates on which atom the basis function is centered and where l describes the character of the atom centered basis function. If we have carbon atoms, for which $Q_\alpha = 4$, l would for instance denote the 4 orbitals $2s$, $2px$, $2py$, $2pz$. Using Equation (64), Equation (63) then simplifies to

$$E_{BS} = Tr[H_0 p(H_0 + U)]. \quad (65)$$

Taking the derivative we get

$$\frac{dE_{BS}}{dR_\alpha} = \sum_\beta \frac{\partial E_{BS}}{\partial u_\beta} \frac{\partial u_\beta}{\partial R_\alpha} + \frac{\partial E_{BS}}{\partial R_\alpha}, \quad (66)$$

where

$$\frac{\partial E_{BS}}{\partial u_\beta} = Tr \left[H_0 p'(H) \frac{\partial H}{\partial u_\beta} \right]. \quad (67)$$

As discussed above, the matrix $p'(H)$ is close to zero in an insulator at sufficiently low temperature and can often be neglected. The forces are therefore approximately given by

$$\frac{dE_{BS}}{dR_\alpha} = \text{Tr} \left[H_0 p(H) \frac{\partial H}{\partial R_\alpha} \right]. \quad (68)$$

It has to be pointed out that to get sufficiently high accuracy the degree of the polynomial has to be higher than in the case of Tight Binding case without local charge neutrality.

The degree n_{pl} of the polynomial needed to represent the Fermi distribution is proportional to

$$\frac{\epsilon_{\max} - \epsilon_{\min}}{\Delta\epsilon}. \quad (69)$$

This follows from the fact, that the n th order Chebychev polynomial has n roots and so a resolution that is roughly proportional to $1/n$. For the usual Tight Binding Hamiltonians the ratio in Equation (69) is not very large and for silicon and carbon systems without gap states polynomials of degree 50 are sufficient. In contexts other than Tight Binding this ratio can however be fairly large and polynomial representation would become very inefficient.

3.1.2 The Rational Fermi Operator Expansion

A rational representation of the density matrix (Goedecker 1995) is in this case more efficient

$$F = \sum_\nu \frac{w_\nu}{H - z_\nu}. \quad (70)$$

As is well known, the function $f(\epsilon)$ given by

$$f(\epsilon) = \frac{1}{2\pi i} \oint \frac{dz}{\epsilon - z} \quad (71)$$

is equal to 1 if ϵ is within the volume encircled by the contour integration path and zero otherwise. If the integration path contains the occupied states as shown in Figure (8) it can therefore be used as a zero temperature Fermi distribution. The exact finite temperature Fermi distribution $f(\epsilon_n(\mathbf{k}))$ can be obtained by replacing the path in this contour integral by a sequence of paths which do not intersect the real axis (Goedecker 1993, Gagel 1998, Nicholson and Zhang 1997). Actually, as already mentioned above, it is usually not necessary to have the exact Fermi distribution. The electronic temperature is just determined by the slope (and possibly some higher derivatives) of the distribution at the Fermi energy. We will also refer to such generalized distributions as Fermi distributions. A distribution of this type can be obtained by discretizing the zero temperature contour integral from Equation (71) as shown in Figure 8.

In principle any other set of z_ν 's and w_ν 's can be used as long as it satisfies

$$f(\epsilon) \approx \sum_{\nu=1}^{n_{pd}} \frac{w_\nu}{\epsilon - z_\nu}, \quad (72)$$

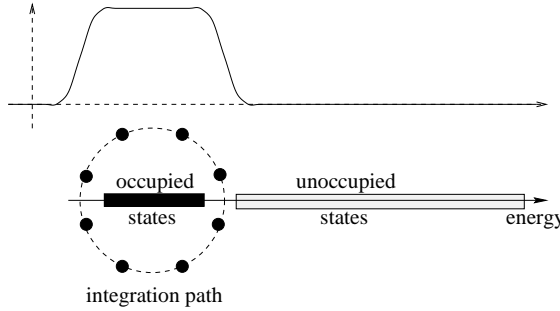


Figure 8: *A discretization of the contour integral in the complex energy plane of Equation (71). The resulting Fermi distribution is shown on top.*

where n_{pd} is the degree of the rational approximation. How can we now evaluate Equation (70) on a computer? Denoting $\frac{I}{H-z_\nu}$ by F_ν we have

$$(H - z_\nu)F_\nu = I \quad (73)$$

$$F = \sum_\nu w_\nu F_\nu. \quad (74)$$

So we have first to invert all the matrices $H - z_\nu$ and then to form linear combinations of them. The inversion is equivalent to the solution of M_b linear systems of equations. This can be effectuated using iterative techniques so that in the end everything can again be done by matrix times vector multiplications. A rational approximation can represent the sharp variation near the chemical potential of a low temperature Fermi distribution in a more efficient way than a Chebychev approximation. Whereas in the Chebychev case the degree of the polynomial is given by Equation (69) the degree of the rational approximation n_{pd} is given by

$$n_{pd} = \frac{\mu - \epsilon_{min}}{\Delta\epsilon}. \quad (75)$$

This n_{pd} in contrast to n_{pl} does not depend on the largest eigenvalue ϵ_{max} . Once n_{pd} is of the order of magnitude given by Equation (75) one has exponential convergence to the zero temperature Fermi distribution. In the case where the integration points and weights are obtained by discretizing the contour integral of Figure 8 this exponential behavior is immediately comprehensible since an equally spaced integration scheme gives exponential convergence for periodic functions (Sloan and Joe, 1994). Since n_{pd} is usually reasonably small, the success of the method will hinge upon whether it is possible to solve the linear system of equations associated with each integration point with a small number of iterations. The number of iterations in an iterative method such as a conjugate gradient scheme (Press *et al.*, 1986) is related to whether it is possible to find a good preconditioning scheme. In the case of plane wave calculations a good preconditioner can be obtained from the diagonal elements and of the order of 10 iterations are required. In other schemes using Gaussians for instance it is not quite clear whether good preconditioners can be found. When the Hamiltonian depends on the atomic positions R_α , Equations (73) and (74) can be differentiated to obtain the derivative $\frac{dF}{dR_\alpha}$, which is needed for the calculation of the forces.

3.2 The Fermi Operator Projection Method

The FOE method is used to calculate the full density matrix. This can be inefficient if the number of basis functions per atom is very large. As was mentioned before, the density matrix at zero temperature does not have full rank. In the case of an insulator it can be constructed from N_{el} Wannier functions (23). If one has a numerical representation of the zero temperature density operator, which is actually a projection operator, that eliminates all components belonging to eigenvalues above the Fermi level, one can apply it to a set of trial Wannier functions \tilde{V}_n , $n = 1, \dots, N_{el}$ to generate a set of orbitals which span the space of the Wannier functions. The numerical representation of the density operator can again either be a Chebychev or rational one. We will first discuss the rational case (Goedecker 1995).

To do the projection with a rational representation, a system of equations analogous to (73) and (74) has to be solved for each trial Wannier function \tilde{V}_n and at each integration point ν

$$(H - z_\nu)\tilde{W}_{n,\nu} = \tilde{V}_n \quad (76)$$

$$\tilde{W}_n = \sum_\nu w_\nu \tilde{W}_{n,\nu}. \quad (77)$$

Thus the saving comes from the fact that one has to solve this system of equations (76) just for N_{el} right hand sides, whereas one has M_b right hand sides in Equation (73). Obviously the solution of the Equation (76) has to be done not within the whole computational volume but only within the localization region to obtain linear scaling. The functions \tilde{W}_n will now span our subspace unless one of our trial functions \tilde{V}_n was chosen in such a way that it has zero overlap with the space of the occupied orbitals, which is highly unlikely. To obtain a set of valid Wannier functions W_n one has still to orthogonalize the orbitals \tilde{W}_n . Since the W_n 's are localized the overlap matrix is a sparse matrix and can be calculated with linear scaling. In the typical Density Functional context, the inversion of this matrix is a rather small part, even if it is done with cubic scaling. In a Tight Binding context it is much more important and a linear scaling method has been devised by Stephan *et al.* (1998) for the inversion. The construction of the Wannier functions by projection according to Equations (76) and (77) is illustrated in Figure 9 in the case of a silicon crystal. In this case one knows that the Wannier functions are bond centered and it is therefore natural to choose a set of bond centered functions as an initial guess. In this example we took simple Gaussians. As shown in Figure 9, the projection modifies the details of the Gaussian but does not significantly change its localization properties.

Chebychev based projection methods have been introduced in connection with other techniques by Sankey *et al.* (1994) and by Stephan *et al.* (1998).

3.3 The Divide and Conquer method

The original formulation of the DC method (W. Yang 1991a, W. Yang 1991b, Zhao and Yang 1995) was based on a subdivision of the electronic density. To calculate the density at a certain point an ordinary electronic structure calculation is done for a sub-volume containing this point. Since the electronic density is only influenced by features in a

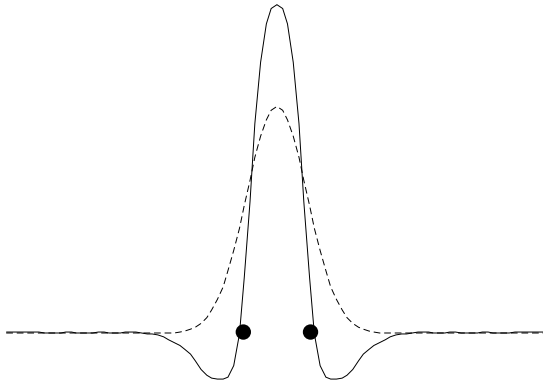


Figure 9: *The effect of applying the density operator, which is a projection operator in the eigenvalue space, to a Gaussian (dashed line) centered in the middle of a bond between two silicon atoms denoted by discs. The resulting function \tilde{W} is shown by the solid line. The orthogonal Wannier function W obtained by symmetric orthogonalization is practically indistinguishable from \tilde{W} on this scale. The calculation was done using Density Functional Theory with pseudopotentials*

rather small neighborhood, the density obtained in this way is a good approximation to the density one would obtain by doing a calculation in the whole volume occupied by the molecule or solid under consideration. The more recent formulation of this theory (W. Yang and T-S. Lee 1995) is however also based on the density matrix and we will discuss this version in more detail. The idea is to calculate certain regions of the density matrix by considering sub-volumes and then to generate the full density matrix by adding up these parts with the appropriate weights. How to calculate the density matrix for the sub-volumes is in principle unspecified but is usually done using ordinary electronic structure calculations based on exact diagonalization. Let us illustrate the principle for synthesizing the density matrix from its subparts in a pictorial way by considering a one-dimensional chain molecule. For simplicity let us also assume that we have atom centered basis functions.

First one divides the whole computational volume into sub-volumes which we will call central regions. Three such central regions are displayed in Figure (10) by dark shading. Around each central region one puts a buffer region denoted by light shading. The sum of these two regions corresponds to the localization region of the other $O(N)$ methods.

Once one has set up this subdivision, one does an electronic structure calculation within each localization region to obtain the density matrix belonging to this region. These different calculations are only coupled by the requirement that the Fermi level is the same in all the localization regions. Typically a very small temperature is used to stabilize the search for the overall Fermi level. From the density matrices obtained in this way, one cuts off all the corners, i.e. the regions where both matrix indices belong to basis functions in the buffer region. This transformation is shown for one localization region in Figure (11).

Using these cross-shaped blocks one then finally synthesizes the density matrix as shown in Figure (12) by adding up the different contributions. The regions shown in dark

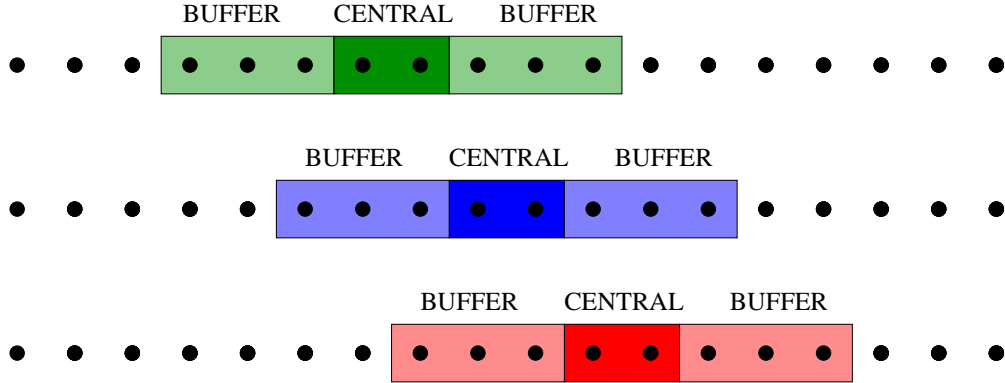


Figure 10: *The different sub-volumes described in the text which are necessary for the application of the DC method to a chain molecule. The atoms are denoted by black dots.*

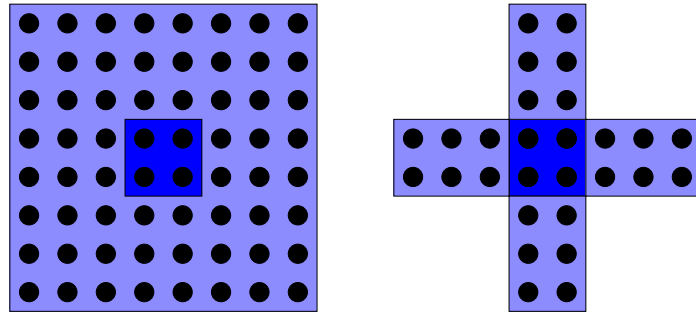


Figure 11: *From the full density matrix calculated for a certain localization region (left hand side) only the cross shaped part (right hand side) is used*

shading which do not overlap with other regions have thereby weight one, whereas the overlapping regions indicated by light shading have each weight one half such that the sum of the weights is one as well in the overlap regions.

The achievement of linear scaling in the DC and OM methods is conceptually related. In both methods certain parts of the density matrix are calculated independently. The main difference is that in the FOE method no calculated parts of the density matrix are discarded in the way done in the DC method as depicted in Figure 11. The FOE method can thus be considered as some DC method where only the central part of the density matrix which is not contaminated by the boundary of the localization region is calculated. The fact that in the DC method only a small part of the density matrix obtained by costly diagonalizations is used, while the largest part associated with the buffer region is thrown away results in a large prefactor (Equation (2)) for this method. This is evidently a particularly serious disadvantage if large localization regions are needed as will be discussed in more detail in section 4.

The calculation of the forces acting on the atoms within the DC method is also described by Yang and Lee (1995). Their force formula is based on the Hellmann-Feynman

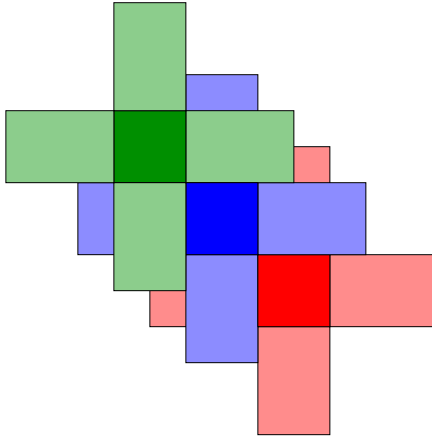


Figure 12: *The full density matrix is obtained by adding up the contributions from the different localization regions. In this figure only 3 contributions from the localization regions of Figure 10 are shown.*

theorem (Feynman 1939) as well as some other terms such as Pulay forces (Pulay 1977) which arise from the use of atom centered basis sets and auxiliary charge densities. As has been discussed in the case of the FOE method the Hellman Feynman expression for the force (56) is not exactly consistent with the total energy expression in a non-variational method, since it is based on the assumption that one is allowed to take traces. Even though the density matrix in the DC method is not calculated via a polynomial expansion, the analysis given for the FOE method also applies to the DC method since conceptually one can represent any matrix functional of H as a polynomial Taylor expansion. The total energy will consequently not have its minimum exactly at the same place where the Hellman Feynman forces vanish if both quantities are calculated with the DC method. In the case of the FOE method there is a simple analytic expression for the calculation of the total energy, even in the case where localization constraints are imposed (Equation (53)). One can therefore differentiate it without using the simplifications arising from the use of traces to obtain consistent forces. No such simple prescription can be written down for the DC method which would allow the calculation of consistent forces. Evidently this compatibility problem becomes negligible for large localization regions and there are certainly practical applications where small inconsistencies of forces and energies are tolerable.

3.4 The Density Matrix Minimization approach

The DMM approach of Li, Nunes and Vanderbilt (1993) is another approach where the full density matrix is constructed. In contrast to the FOE method one obtains the density matrix F in the limit of zero temperature, so no adjustable temperature parameter enters the calculation. The density matrix is obtained by minimizing the following functional for the grand potential Ω with respect to F

$$\Omega = \text{Tr}[(3F^2 - 2F^3)(H - \mu I)] . \quad (78)$$

There is no constraint imposed during the minimization so all the matrix elements of F are independent degrees of freedom. Nevertheless the final density matrix will obey the correct constraint of being a projector if no localization constraints are imposed. This is related to the fact that the matrix $3F^2 - 2F^3$ is a purified version of F as can be seen from Figure 13. If F has eigenvalues close to zero or one then the purified matrix will have eigenvalues that are even closer to the same values. It is also clear from Figure 13 that the eigenvalues of the purified matrix are contained in the interval $[0;1]$ as long as the eigenvalues of F are in the interval $[-1/2 ; 3/2]$.

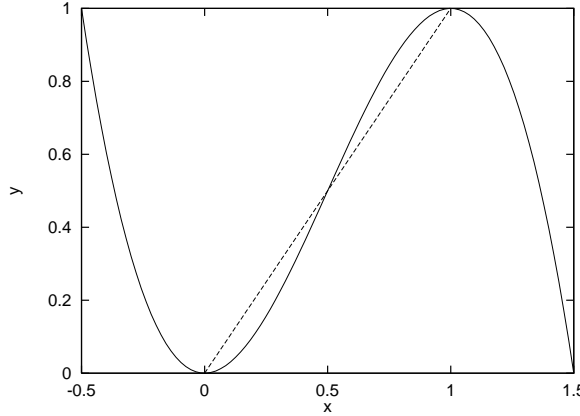


Figure 13: *The McWeeny (1960) purification function $3x^2 - 2x^3$*

The gradient of Ω as given by Equation (78) with respect to F is itself a matrix and it is given by

$$\frac{\partial \Omega}{\partial F} = 3(F H' + H' F) - 2(F^2 H' + F H' F + H' F^2), \quad (79)$$

where $H' = (H - \mu I)$. In order to verify that Equation (78) defines a valid functional we have to show two things. First, that the grand potential expression (78) gives the correct result if we insert the exact density matrix F , and second, that the gradient (79) vanishes in this case. From Equation (24) we see that the exact F is a projection operator, i.e. that $F^2 = F$. Therefore $(3F^2 - 2F^3) = F$ and the grand potential expression (78) agrees indeed with the correct result (11). Using in addition the fact that H' and the exact F commute (as follows from Equations (20), (21)) it is also evident that the gradient in Equation (79) vanishes. The gradient vanishes however not only for the ground state density matrix F but also for any excited state density matrix. In order to exclude the possibility of local minima, we have to verify, that these stationary points are no minima. This can easily be done (D. Vanderbilt, private communication) using the fact that the functional is a cubic polynomial with respect to all its degrees of freedom. Let us suppose that there are two minima. Inspecting the functional along the line connecting these two minima we would obviously again find these two minima, which is a contradiction because a cubic polynomial cannot have two minima. Thus we have proved by contradiction that the DMM functional has only one single minimum.

There is a second thing which is worrying at first sight with this functional. If the density matrix for an insulator at zero temperature is of the correct form (i.e. if the occupation numbers n_l are integers) the gradient (79) will vanish independently of the value of the chemical potential. This ambiguity however disappears as soon as one has fractional occupation numbers. Let us consider an approximate density matrix of the form

$$F = \sum_l n_l |\Psi_l \rangle \langle \Psi_l|. \quad (80)$$

Then it is easy to see that

$$\Omega = \sum_l (\epsilon_l - \mu)(3n_l^2 - 2n_l^3) \quad (81)$$

$$\frac{\partial \Omega}{\partial F} = \sum_l 6(\epsilon_l - \mu)n_l(1 - n_l)|\Psi_l \rangle \langle \Psi_l|. \quad (82)$$

The polynomial of Equation (81) is the same as the one shown in Figure 13 and we see that components corresponding to eigenvalues larger than the chemical potential are damped until they vanish in the minimization process, whereas components corresponding to smaller eigenvalues are amplified until they reach the value one. Thus the chemical potential will determine the number of electrons to be found in the system as it should. The above statements are actually only correct if all the n_l 's are contained in the interval $[-1/2, 3/2]$. If this is not the case then one can see from Figure 13, that there can be runaway solutions, where some n_l tend to $\pm\infty$. When we implemented the scheme we however never encountered in practice such a runaway case.

Having convinced ourselves, that the functional defined in Equation (78) is well behaved, let us now estimate the number of iterations which are necessary to minimize it. As is well known, the error reduction per iteration step depends on the condition number κ which is the ratio of the largest curvature a_{max} to the smallest curvature a_{min} at the minimum. These curvatures could be determined exactly by calculating the Hessian matrix at the minimum. Let us instead only derive an estimate of these curvatures by calculating the curvature along some representative directions. To do this let us now consider a ground state density matrix where some fraction x of an excited state is mixed in

$$F(x) = \sum_{n=1}^{N_{el}} \Psi_n^*(\mathbf{r}) \Psi_n(\mathbf{r}) - x \Psi_I^*(\mathbf{r}) \Psi_I(\mathbf{r}) + x \Psi_J^*(\mathbf{r}) \Psi_J(\mathbf{r}). \quad (83)$$

The index I is a member of the N_{el} eigenstates below μ and the index J refers to a state above μ . The expectation value of the OM functional for this density matrix is given by

$$\begin{aligned} \Omega(x) &= \text{Tr}[(3F(x)^2 - 2F(x)^3)(H - \mu I)] \\ &= \sum_{n=1}^{N_{el}} \epsilon_n + (3x^2 - 2x^3)(\epsilon_J - \epsilon_I) \end{aligned} \quad (84)$$

and its second derivative by

$$\left. \frac{\partial^2 \Omega(x)}{\partial x^2} \right|_{x=0} = 6(\epsilon_J - \epsilon_I). \quad (85)$$

The largest curvature will roughly be $\epsilon_{max} - \epsilon_{min}$ and the smallest curvature of the order of the HOMO-LUMO separation $\epsilon_{gap} = \epsilon_{N_{el}+1} - \epsilon_{N_{el}}$. The condition number is thus given by

$$\kappa = \frac{a_{max}}{a_{min}} \approx \frac{\epsilon_{max} - \epsilon_{min}}{\epsilon_{gap}}. \quad (86)$$

In the conjugate gradient method, which is the most efficient method to minimize the DMM functional, the error e_k decreases as follows (Saad)

$$e_k \propto \left(\frac{\sqrt{\kappa} - 1}{\sqrt{\kappa} + 1} \right)^k. \quad (87)$$

The error e_k is defined in this context as the length of the vector which is the difference between the exact and approximate solution at the k -th iteration step. Under realistic conditions κ is large and the number of iterations n_{it} to achieve a certain accuracy is therefore proportional to

$$n_{it} \propto \sqrt{\kappa} = \sqrt{\frac{\epsilon_{max} - \epsilon_{min}}{\epsilon_{gap}}}. \quad (88)$$

This is an important result since it indicates that in an insulator the number of iterations is independent of system size. This result is also confirmed by numerical tests.

The use of a conjugate gradient scheme requires line minimizations along these conjugate directions. For arbitrary functional forms this has to be done by numerical techniques such as bisection (Press *et al.*, 1986). In the case of the DMM functional we have however a cubic form along each direction. The four coefficients determining the cubic form can be calculated with four evaluations of the functional. Once these 4 coefficients are known the minimum along this direction can easily be found.

Doing a series of minimization steps as outlined above will in general result in a density matrix which does not lead to the correct number of electrons. Thus one has to do some outer loops where one searches for the correct value of the chemical potential. For better efficiency, these two iterations loops can however be merged into one loop where one alternatingly minimizes the energy and adjusts the chemical potential (S-Y. Qui *et al.*, 1994).

The forces on the atoms are given by

$$\frac{d\Omega}{dR_\alpha} = \frac{\partial\Omega}{\partial F} \frac{\partial F}{\partial R_\alpha} + \frac{\partial\Omega}{\partial H} \frac{\partial H}{\partial R_\alpha}. \quad (89)$$

Since the method is variational, $\frac{\partial\Omega}{\partial F}$ vanishes at the solution and the force formula simplifies to

$$\frac{d\Omega}{dR_\alpha} = \frac{\partial\Omega}{\partial H} \frac{\partial H}{\partial R_\alpha} = Tr \left[(3F^2 - 2F^3) \frac{\partial H}{\partial R_\alpha} \right] \quad (90)$$

which can easily be evaluated.

The introduction of a localization region leads again to some subtleties. Whereas in the unconstrained case the eigenvalues of the final density matrix F will all be either zero or one, this is not any more the case when a localization region is introduced. So the

truncated F is not any more a projection matrix but it is given by

$$F = \sum_{m=1}^{M_b} n_m \Psi_m^*(\mathbf{r}) \Psi_m(\mathbf{r}), \quad (91)$$

where now Ψ_m are the eigenfunctions of the truncated F and the occupation numbers n_m their eigenvalues. In a certain sense the localization constraint introduces a finite electronic temperature. This is actually not surprising after the discussion of the relation between the temperature and the localization properties in section 2. Figure 14 shows the energy expectation values of the eigenvectors of F versus the occupation numbers, for the case of a crystalline Si cell of 64 atoms, where the localization region extends up to the second nearest neighbors. As one sees, the energy expectation values $\langle \Psi_m | H | \Psi_m \rangle$ of the eigenvectors of F are very close to the exact eigenvalues of H .

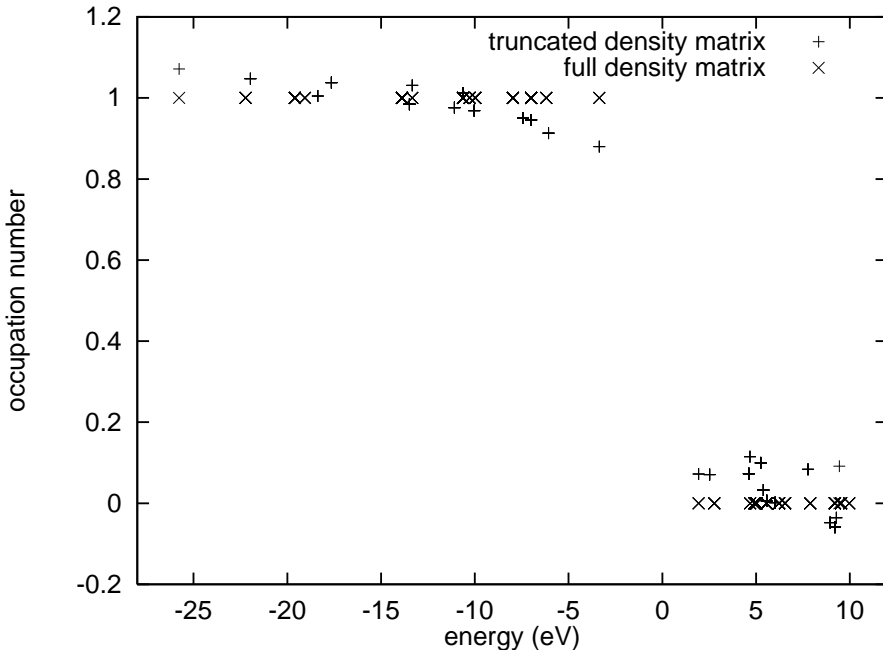


Figure 14: *An analysis of the eigenvectors of the full and truncated density matrix. In the case of the full density matrix the eigenvectors were chosen to be simultaneously eigenvectors of both F and H , and the eigenvalues with respect to F (occupation numbers) are plotted versus the eigenvalues with respect to H . In the case of the truncated density matrix, the eigenvectors cannot anymore simultaneously diagonalize F and H . Therefore the eigenvalues with respect to F are plotted versus their energy expectation values with respect to H . Note that in the energy expression (78) the purified density matrix $3F^2 - 2F^3$ enters instead of F . The occupation numbers of the purified version are closer to zero or one.*

This close correspondence of the eigenvectors of F to the eigenvectors of H explains why the number of iterations needed to find the minimum does not increase as one introduces localization constraints. Equation (85) remains approximately valid if the occupation numbers for the occupied states are close to 1 and if the occupation numbers for the

unoccupied states are very small as well as if the energy expectation values $\langle \Psi_m | H | \Psi_m \rangle$ are close to the exact eigenvalues of the Hamiltonian. These conditions are fulfilled as discussed above. Hence the condition number for the minimization process does not change appreciably in the truncated case.

All the arguments used to prove the absence of local minima remain valid in the truncated case as well. The force formula Equation (90) remains equally valid.

An alternative derivation of this algorithm has been given by Daw (1993). He considers a differential equation which describes the evolution of a density matrix when the electronic temperature is cooled down from infinity to zero. The change of the density matrix during this process is equal to the gradient of Equation (79).

3.5 The Orbital Minimization approach

The OM method (Mauri *et al.*, 1993, Ordejon *et al.*, 1993, Mauri and Galli 1994, Ordejon *et al.*, 1995, Kim *et al.*, 1995) also calculates the grand potential in the limit of zero temperature. In contrast to the two previous methods, it does not calculate the density matrix directly but expresses it via the Wannier functions according to Equation (23). These Wannier functions are obtained by minimizing the following unconstrained functional.

$$\Omega = 2 \sum_n \sum_{i,j} c_i^n H'_{i,j} c_j^n - \sum_{n,m} \sum_{i,j} c_i^n H'_{i,j} c_j^m \sum_l c_l^n c_l^m, \quad (92)$$

where c_i^n is the expansion coefficient of the n -th Wannier orbital with respect to the i -th basis function and $H'_{i,j}$ are the matrix elements of the shifted Hamiltonian $H - \mu I$ with respect to the basis functions. In the original formulation (Mauri *et al.*, 1993, Ordejon *et al.*, 1993, Mauri and Galli 1994, Ordejon *et al.*, 1995) only N_{el} orbitals were included in the orbital sums in Equation (92) (i.e. $n = 1 \dots N_{el}$, $m = 1 \dots N_{el}$). In the formulation of Kim (1995) more than N_{el} orbitals are included in the sums. The functional of Equation (92) can be derived by considering the ordinary band structure energy expression

$$E_{BS} = \sum_n \sum_{i,j} c_i^n H'_{i,j} c_j^n \quad (93)$$

and by incorporating the orthogonality constraint by a Taylor expansion of the inverse of the overlap matrix O between the occupied orbitals

$$O_{n,m} = \sum_l c_l^n c_l^m \quad (94)$$

up to first order. A family of related functionals can be obtained by Taylor expansions to higher order (Mauri and Galli 1994, Galli 1996). Since these functionals do not offer any significant advantage and are not used in calculations we will not discuss them. The gradient of the functional of Equation (92) is given by

$$\frac{\partial \Omega}{\partial c_k^n} = 4 \sum_j H'_{k,j} c_j^n - 2 \sum_m \sum_j H'_{k,j} c_j^m \sum_l c_l^n c_l^m - 2 \sum_m c_k^m \sum_{i,j} c_i^n H'_{i,j} c_j^m. \quad (95)$$

Let us first discuss this functional in the case where no localization constraint is imposed on the orbitals. It is easy to see that the functional (92) is invariant under unitary transformations of the occupied (i.e. N_{el} lowest) orbitals. So we can derive our results in terms of eigenorbitals rather than Wannier orbitals. The coefficients c_i^n are then the expansion coefficients of the eigenorbitals. Using the fact that in this case $\sum_l c_l^n c_l^m = \delta_{n,m}$ and that $\sum_{i,j} c_i^n H'_{i,j} c_j^m = \delta_{n,m}(\epsilon_n - \mu)$ we obtain

$$\begin{aligned}\Omega &= 2 \sum_n \sum_{i,j} c_i^n H'_{i,j} c_j^n - \sum_{n,m} \sum_{i,j} c_i^n H'_{i,j} c_j^m \delta_{n,m} \\ &= \sum_n \sum_{i,j} c_i^n H'_{i,j} c_j^n \\ &= \sum_n \epsilon_n - \mu N_{el}\end{aligned}$$

which is the standard expression (11) for the grand potential. Similarly the gradient expression can be simplified obtaining

$$\begin{aligned}\frac{\partial \Omega}{\partial c_k^n} &= 4 \sum_j H'_{k,j} c_j^n - 2 \sum_m \sum_j H'_{k,j} c_j^m \delta_{n,m} - 2 c_k^n \sum_m \delta_{n,m}(\epsilon_m - \mu) \\ &= 2 \sum_j H'_{k,j} c_j^n - 2 c_k^n (\epsilon_n - \mu) = 0.\end{aligned}\quad (96)$$

So the functional has indeed a vanishing gradient at the ground state and it gives the correct ground state energy. As was the case for the DMM functional the gradient vanishes not only for the set of ground state orbitals but also for any set of excited states. So we have to verify that these stationary points are not local minima but saddle points. We do this by picking a certain direction along which the curvature is negative. In the OM case an excited state is described by a set of N_{el} orbitals Ψ_n where at least one index $n = I$ corresponding to an occupied orbital I is replaced by an unoccupied orbital J . Let us now consider the variation of the grand potential $\Omega(x)$ under a transformations of the form $\Psi_J \rightarrow \cos(x)\Psi_J + \sin(x)\Psi_I$. One can show that the curvatures at these stationary points is given by

$$\left. \frac{\partial^2 \Omega(x)}{\partial x^2} \right|_{x=0} = -4(\epsilon_J - \epsilon_I). \quad (97)$$

Since the unoccupied eigenvalue ϵ_J is higher in energy than the occupied one ϵ_I , the curvature is negative and we have indeed a saddle point. In the same way we can also again show that the condition number is given by Equation (86).

Also in analogy to the DMM functional one can show (Kim *et al.*, 1995) that in the formulation of Kim, the chemical potential μ determines the number of electrons by amplifying components below μ and annihilating components above it. Considering a state consisting of a set of eigenfunctions Ψ_n of H where each eigenfunction is multiplied by a scaling factor a_n , the expectation value for the grand potential becomes

$$\Omega = \sum_n (2 - a_n^2) a_n^2 (\epsilon_n - \mu). \quad (98)$$

The relevant function $(2 - x^2)x^2$ is shown in Figure (15). One can see that the minimum of Equation (98) is attained by $a_n = 0$ if $\epsilon_n > \mu$ and by $a_n = \pm 1$ if $\epsilon_n < \mu$. Again

this is only true if a_n is within a certain safety interval. Otherwise there can be runaway solutions. Infinitesimally close to the solution μ becomes ill defined in an insulator as it should.

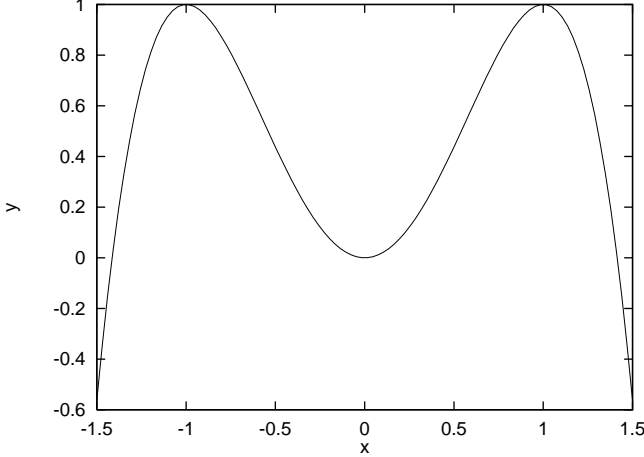


Figure 15: *The function $(2 - x^2)x^2$ relevant in Equation (98)*

Whereas the DMM functional keeps all its good properties when one introduces a localization constraint, the OM functional loses most of them. The localization constraint is introduced in the OM functional by allowing each Wannier orbital to deviate from zero only within its own localization region. These localization regions are usually atom centered and contain a few shells of neighboring atoms. The basic idea of the OM functional, namely of describing an electronic system by a set of Wannier functions with finite support is already problematic. Orthogonality and finite support are mutually exclusive properties and so the orbitals which one obtains in the minimization process are necessarily non-orthogonal. The true Wannier functions are however orthogonal. In addition, as we have seen in the DMM case, a density matrix which is truncated has full rank, i.e. none of its eigenvalues is exactly zero. Thus N_{el} Wannier orbitals are not sufficient to represent the density matrix in this case. The generalized formulation of Kim (1995) where more than N_{el} orbitals are used alleviates this problem, but does not completely fix it unless the number of orbitals is equal to the number of basis functions M_b .

When implemented with localization constraints the OM functional exhibits the following problems:

- The functional has multiple minima (Ordejon *et al.*, 1995). Depending on the initial guess one obtains thus different answers, some of which are physically meaningless (Kim 1995). As we have shown above in Equation (97) the functional has no multiple minima in the non-truncated case. The analysis we used to show this was based on the eigenfunctions. Since the Wannier functions have no resemblance to the eigenfunctions this analysis cannot be carried over into the localized regime. In the case of the DMM method the absence of multiple minima could be proven using the fact that the DMM functional is cubic. The OM functional (92) is however quartic with respect to its degrees of freedom and will thus in general have multiple minima.

The problem of the multiple minima is attenuated by the formulation of Kim (1995) but it is not completely eliminated since the functional still has quartic character. As a byproduct of the multiple minimum problem, the total energy cannot be conserved in molecular dynamics simulations, which is an important requirement. Here again, energy conservation is better in the Kim formulation but still far from perfect (Kim 1995).

In practical applications of the OM method for electronic structure methods great care is usually taken to construct input guesses which correspond to the physical bonding properties of the molecule under consideration (Itoh *et al.*, 1996). If the minima that is closest in distance is always selected during the subsequent line minimizations then one will most likely end up in a physically reasonable minima that reflects the bonding properties of the input guess (Stephan private communication). This is especially true if the localization regions are large and if the topology of the total energy surface within a reasonably large region around the physical minimum is not too different from the one of the non-truncated case. Such a procedure is of course not applicable in systems where the exact bonding properties are unknown.

- The number of iterations is very large whenever any localization constraint is imposed together with tight convergence criteria. This is due to the deterioration of the condition number, a phenomenon which is easy to understand (Ordejon 1995). Introducing a localization region destroys the strict invariance of the band structure energy under unitary transformations among the occupied orbitals. When the localization region is large, this invariance will still approximately exist and one can find certain directions around the minimum where the energy varies extremely slowly and where the curvature is therefore much smaller than the smallest curvature ϵ_{gap} in the unconstrained case. Whereas directions where the curvature is strictly zero do not affect the condition number, these very small curvatures will have a negative effect on the condition number (Equation (86)) and the required number of iterations is consequently much larger in the constrained case than in the unconstrained case. Even though the condition number deteriorates with increasing localization region, the detrimental effect on the number of iterations will disappear at a certain point where the gradient due to these small curvatures becomes smaller than the numerical threshold determining the convergence criterion of the minimization procedure.
- The optimal localization regions would be centered on the centers of the Wannier functions. Since these centers are not known a priori, atom centered localization regions are usually chosen. In this case the Wannier functions do not generally exhibit the correct symmetry (Ordejon 1995). As a consequence molecular geometries obtained from this functional can have broken symmetry as well. In a C_{60} molecule for instance there are only two equivalent sites. When treated with the OM functional they are however all slightly different (Kim *et al.*, 1995).
- As follows from Equation (98) there can be runaway solutions. We have encountered this problem in test cases with random numbers as input guess. If one would construct a more sophisticated input guess, based on the bonding properties of the

system, this would however probably not occur. In the DMM method the possibility of runaway solutions also exists but is never found in practice even with the most trivial input guess.

- If the method is used in the context of self-consistent calculations, where the electronic charge density is used to calculate the Hartree and exchange correlation potential, problems arise, since the total charge is not conserved during the minimization iteration (Mauri and Galli 1994).

To overcome the competing requirements of orthogonality and localization, a related approach has recently been proposed by Yang (1997) where the orbitals are allowed to be non-orthogonal. This approach of Yang has up to now not been applied in connection with a localization constraint.

3.6 The Optimal Basis Density Matrix Minimization method

Despite its many advantages in the Tight Binding context, the DMM method has the big disadvantage that it is very inefficient if one needs very large basis sets (i.e. many basis functions per atom). Large basis sets are typically required in grid based Density Functional calculations. In this case it just becomes impossible to calculate and store the full density matrix in the DMM method even though it is a sparse matrix. From this point of view the Wannier function based methods are advantageous since they do not require the full density matrix. The basic idea of the OBDMM method (Hierse and Stechel 1994, Hernandez and Gillan 1995) is now to contract first the fundamental basis functions into a small number of new basis functions and then to set up the Hamiltonian and overlap matrix in this new small basis. A generalized version of the DMM method which can be applied to the non-orthogonal context (a subject which will be discussed later in the article) is then used to solve the electronic structure problem in this basis. The essential point is that one tries to do the contraction in an optimal way. This is done by minimizing the total energy also with respect to the degrees of freedom determining the contracted basis functions Ψ_n . Formulated mathematically the density matrix is given by

$$F(\mathbf{r}, \mathbf{r}') = \sum_{i,j} \Psi_i^*(\mathbf{r}) K_{i,j} \Psi_j(\mathbf{r}') . \quad (99)$$

The matrix K is a purified version of the the density matrix within the contracted basis L and it is given by

$$K = 3LOL - 2LOLOL , \quad (100)$$

where O is the overlap matrix among the contracted orbitals. The main difference between the formulation of Hierse and Stechel and of Hernandez and Gillan is that in the first formulation the number of contracted basis functions Ψ_i is equal to the number of electrons, whereas in the second approach it can be larger. In the formulation of Hernandez and Gillan the basis set can for instance be chosen to have the size of a minimal basis set. The difference to standard minimal basis sets from quantum chemistry is that it is optimally adapted to its chemical environment since the contraction coefficients are not predetermined but found variationally. In practice the full density matrix is found

by a double loop minimization procedure. In the inner loop one has the ordinary DMM procedure to find the density matrix for a given contracted basis set. In the outer loop one searches for the optimally contracted basis functions Ψ_i for fixed L .

Unfortunately the minimization of the contracted basis functions Ψ_i is ill conditioned (Gillan *et al.*, 1998) and the number of iterations is therefore at present very large. As already explained before ill-conditioning occurs if the curvatures in the minimum along different directions are widely different. Three causes for the ill-conditioning are reported by Gillan (1998).

- Length scale ill-conditioning:

This problem is actually not related to the OBDMM algorithm itself but to the (uncontracted) basis functions which are taken to be so-called "Blip" functions in the present implementation. This kind of problem can be found in all iterative electronic structure algorithms if grid based basis functions such as finite elements are used. Its origin is easy to understand. Let us imagine that we are searching for the lowest state of jellium using a localized basis set associated with an equally spaced grid. By symmetry the solution is a constant vector, i.e. all basis functions have the same amplitude in the solution vector. Let us now assume that we explore the energy surface around the minimum along several directions. Let us first "go" into a direction where we add components in such a way that the sign of the amplitude of each neighboring basis function changes. This corresponds to a high frequency plane wave and since the kinetic energy of such a plane wave is big, the total energy will rapidly increase if we add a such a contribution to our solution vector. If on the other hand we add contributions that correspond to low frequency plane waves the energy will increase much more slowly. Since in grid based methods the basis functions are usually narrow and since one can thus construct high frequency functions the condition number can be very bad. As one can suspect from the above explanation the different curvatures can be estimated by doing a Fourier analysis. With this information one can then use preconditioning techniques to cure the length scale ill-conditioning problem. Such a scheme has been proposed by Bowler and Gillan (1998).

- Superposition ill-conditioning:

This ill-conditioning problem is essentially identical to the ill-conditioning problem of the OM functional. If we have N_{el} contracted basis functions and no localization constraints the total energy is invariant with respect to unitary transformations of these functions. The introduction of a localization constraint destroys this invariance but there is an approximate invariance left with manifests itself in very small curvatures in the minimum along certain directions.

- Redundancy ill-conditioning:

This problem can only be found in the formulation of Hernandez and Gillan, where the number of contracted basis functions is larger than the number of electrons. In this case one spans a space that contains not only the occupied orbitals but also some unoccupied. As was shown before in the context of the DMM functional introducing a localization constraint will not assign zero occupation numbers, but only very small

occupation numbers to components corresponding to the unoccupied states in the unconstrained case. Since these components corresponding to the unoccupied states have now very little weight they have little influence on the total energy and one has again certain directions where the total energy changes very slowly resulting in very small curvatures.

Another open question is whether the OBDMM has local minima. The functional is a 6-th order polynomial with respect to the expansion coefficients of the contracted basis functions as can be seen from Equation (99) and (100). The two overlap matrices in Equation (100) give each a quadratic term, the two contracted orbitals in Equation (99) a linear term. Minimization with respect to the contracted basis functions should therefore exhibit local minima. Local minima have however not been reported with this method so far. Perhaps the following DMM minimization step which is free of local minima saves the method from overall local minima.

4 Comparison of the basic methods

It is certainly not possible to claim that a specific method is the best for all applications. Nevertheless the methods presented so far differ in many respects and one can therefore clearly judge under which limiting circumstances certain methods will fail or perform well. In the following the methods presented so far will therefore be compared under several important aspects. The comparison will be done in two categories. The first category applies to electronic structure methods requiring a small number of degrees of freedom per atom. The Tight Binding method belongs to the first category requiring a few basis functions per atom (or just a few degrees of freedom in the case of semiempirical Tight Binding). But we will also include the standard quantum chemistry methods into this first category, where one typically needs from a few up to a few dozen Gaussian type basis functions per atom. The second category contains methods which are grid based such as finite difference schemes (Chelikowsky *et al.*, 1994), or where the basis functions can be associated with grid points such as in finite element basis functions (White *et al.*, 1989) or blip (Hernandez *et al.*, 1997) basis functions. In these methods one has typically many hundred degrees of freedom per atom. Even though the density matrix is a sparse matrix, $O(N)$ methods which calculate the full density matrix can not be applied to the second category of electronic structure methods. The memory requirements alone are already prohibitive. As pointed out before we can expect that the localization region in a 3-dimensional structure comprises on the order of 100 atoms. The density matrix will exhibit significant sparseness only for larger system. Assuming that we just have 100 basis functions per atom the storage of the density matrix would require about 1 Gigabyte of memory which is the upper limit of current workstations. The comparison in the large basis set class will therefore comprise only the methods which are Wannier function based namely FOP, OM and OBDMM. The comparison in the small basis set class will comprise FOE, DC, DMM and OM, excluding two methods which are explicitly targeted at large basis sets, namely FOP and OBDMM.

4.1 Small basis sets

The comparison of the methods applicable to small basis sets is based on the following criteria:

- Scaling with respect to the size of the localization region:

The size of the localization region is taken as the number of atoms contained within it. Only the FOE method has a linear scaling with respect to the size of the localization region. As one increases the size of the localization region the nonzero part of each column of the Chebychev matrices increases linearly implying also a linear increase in the basic matrix time vector multiplication part. In the DMM method the CPU time increases quadratically since the numerical effort for the basic matrix times matrix multiplications grows quadratically with respect to the number of off-diagonal elements of the matrix. Neglecting ill-conditioning problems, the OM method exhibits quadratic scaling, since the numerical effort for the calculation of the overlap matrix (Equation (94)) between the Wannier orbitals increases quadratically. As the localization region grows there are more matrix elements and the calculation of each matrix element is more expensive since each orbital is described by a longer vector. Because the ill-conditioning problem becomes more severe for large localization regions the number of iterations increases in reality in a way which is difficult to model resulting in an effective scaling that is stronger than linear. The DC method has a cubic scaling with respect to the size of the localization region if each sub-volume is treated with diagonalization schemes. From the comparison of the scaling behavior of all these methods one can thus conclude, that the FOE method will clearly perform best if large localization regions are needed. The FOE method is thus also the only method which can be faster than traditional cubically scaling algorithms if no localization constraints are imposed. In this case its overall scaling behavior is quadratic whereas all other methods have a cubic scaling with a prefactor which is significantly larger than the one for exact diagonalization.

- Scaling with respect to the accuracy:

A detailed comparison of the polynomial FOE method and the DMM method under this aspect has recently been given by Baer and Head-Gordon (1997) for systems of different dimensionality. Their analysis is based on the assumption that the decay constant γ is given by the tight binding limit of Equation (37). They conclude, that in the one dimensional case the DMM has the best asymptotic behavior, but its prefactor is much larger than the one of the FOE method, so that the FOE method is more efficient in the relevant accuracy regime. In the two dimensional case they have the same asymptotic behavior, but the FOE method has again a much smaller prefactor. In the most relevant three dimensional case the FOE method has both the best asymptotic behavior and prefactor. These results are plausible after the preceding discussion of the scaling with respect to increasing localization region size. When one wants to improve the accuracy the most important factor is the enlargement of the localization region. It is also clear that in higher dimensions the number of atoms within the localization region grows faster than in lower dimensions and that the scaling with respect to the number of atoms will thus become the

decisive factor in 3 dimensions. In lower dimensions the number of iterations has higher relative importance, favoring the DMM method. A comparison of the FOE and DMM method applied to quasi two-dimensional huge tight binding fullerenes by Bates and Scuseria (1998) is also in agreement with the above statements. They found that the FOE and DMM methods give nearly the same performance with a small advantage for the FOE method.

As discussed before, the scaling of the OM and DC methods is stronger than quadratic with respect to the size of the localization region. It is therefore clear that the required numerical effort for increased accuracy will grow even faster than in the DMM method.

- Scaling with respect to the size of the gap:

In the FOE method the degree n_{pl} of the Chebychev polynomial increases linearly with decreasing gap (Equation (69)). At the same time the density matrix decays more slowly. It follows from Equation (37) that the linear extension of the localization region grows as ϵ_{gap}^{-1} in the applicable weak binding limit. The volume of the localization region and the number of atoms contained in it grow consequently as ϵ_{gap}^{-3} . Taking into account the number of iterations (Equation (69)), the total numerical effort increases thus as ϵ_{gap}^{-4} . In the DMM method the number of iterations also increases with decreasing gap but more slowly namely like $\epsilon_{gap}^{-1/2}$ as follows from Equation (88). Taking into account the above discussion of the scaling properties of the DMM method with increasing localization region we obtain the overall scaling of $\epsilon_{gap}^{-13/2}$, which is higher than the scaling behavior of the FOE method. Obviously the scaling behavior of the OM and DC methods is worse. So in contrast to what one might first think the FOE methods performs best in this limit. In three-dimensional metallic systems, the FOE method is thus to be expected to be the only method which will work efficiently at good accuracies.

- Finding a first initial guess:

No initial guess is required in the FOE and DC methods (except perhaps for the potential in a selfconsistent calculation). In the DMM method an extremely simple and efficient input guess for the density matrix is just a diagonal matrix that sums up to the correct number of electrons. In the OM method this point is somewhat problematic. As mentioned above a Wannier function represents typically a bond or lone electron pair. So if one can draw the standard Lewis structure of a molecule, where bonds are denoted by lines and a lone electron pair by a pair of dots, one knows where the Wannier functions should be centered and the Lewis formula can be the basis for the initial guess. This procedure can not be used any more if the molecule is characterized by two or more Lewis structures that are resonating. Especially if the two Lewis structures correspond to an electron transfer over a distance which is larger than the range of the localization region, serious problems are to be expected with Wannier function based methods. In such a case it might actually not only be impossible to find an initial guess, but it might also be impossible at all to describe such a molecule by N_{el} localized Wannier functions.

- Number of iterations in electronic structure calculations:

In the variational methods (OM, DMM) the number of iterations depends on the condition number of the energy expression. As pointed out the OM energy expression is ill conditioned under localization constraints and therefore the required number of iterations is very large. Even for modest accuracy several hundred iterations are required (Mauri and Galli 1994, Ordejon *et al.*, 1995). In the DMM method on the other hand the number of iterations is equal to the number of iterations one needs in ordinary electronic structure calculations (non $O(N)$), namely 20 to 30 (Nunes private communication). The quantity that corresponds to the number of iterations in the FOE method is the degree n_{pl} of the polynomial. While it is difficult to compare the cost of one Chebychev recursion step with the cost of a DMM minimization step, such a comparison can be done in the case of the OM method. In each OM line minimization step one has to calculate the minimum of a quartic polynomial which requires at least 3 applications of H to the wavefunction. One Chebychev recursion step requires one application of H .

- Number of iterations in molecular dynamics simulations:

In molecular dynamics simulations as well as structural relaxations steps and self-consistent mixing schemes the density matrix or respectively the Wannier functions from the previous step are a good input guess for the next step. Good initial input guesses are beneficial in all methods except in the polynomial FOE method and the DC method. It is difficult to quantify the possible savings of such a reuse. To preserve the quality of the solution of the preceeding step as an input guess in a Molecular Dynamics simulation, it can be necessary to make the time step smaller than the integration scheme would allow. How large the maximum time step can be depends of course also on the order and properties of the time integration scheme used to propagate the Molecular Dynamics simulation. Similar remarks apply to the case of structural relaxations. The decisive factor determining the number of iterations per molecular dynamics step is in this context again the condition number of the functional. With the DMM methods of the order of 2 to 3 steps are needed both for accurate molecular dynamics simulations (Qiu 1994) and for structural relaxations (Nunes private communication). The smallest number of iterations that was used in molecular dynamics simulations with the OM method was 10, but at the price of a very poor energy conservation.

- Cross over point for standard Tight Binding systems:

The FOE method has the lowest reported cross over point for the standard carbon test-system in the crystalline diamond structure. For the FOE method it is around 20 atoms (Goedecker 1995), and for the DMM it is estimated (Li *et al.*, 1993) to be around 90 atoms. No crossover points were ever given for the OM and DC method and presumably they are much higher. All quoted cross over points for electronic structure calculations are for an accuracy of roughly 1 percent in the cohesive energies, but in the relevant publications not all computational details are listed to ensure that these numbers are really comparable in all respects. The low crossover point of the FOE method can be understood in terms of its scaling behavior with respect to the size of the localization region discussed above. For small systems the size of the localization region equals the size of the whole system.

The FOE method therefore starts off with a quadratic scaling behavior, whereas all other methods start off with a cubic behavior. Consequently the cross over point for all other methods can only be for system sizes larger than the localization region, whereas the crossover point in the FOE method can already be at smaller system sizes if it is implemented efficiently.

In the context of molecular dynamics simulations the cross over points are different because some of the variational methods can benefit from good input guesses. For the FOE method the cross over point remains at 20 atoms, for the OM method Mauri and Galli quote 40 atoms, and for the DMM method Qui *et al.* (1994) quote 60 atoms. Again no crossover point is given for the DC method. It has to be stressed however that the number quoted by Qui *et al.*, (1994) was for highly accurate molecular dynamics runs where the total energy was conserved, while in the benchmarks of Mauri and Galli no satisfactory energy conservation was obtained.

- Influence of the range of a sparse Hamiltonian matrix on the performance:

In the FOE method the numerical effort increases strictly linearly with respect to the number of nonzero elements per column which depends cubically on the range of the Hamiltonian matrix. In the case of the DMM method it can be shown (Li *et al.*, 1993) that one has to calculate intermediate product matrices only up to a range which is the sum of the range of the density matrix and the Hamiltonian matrix. As long as the range of the Hamiltonian is small compared to the range of the density matrix the number of operations increases therefore only very weakly with respect to an increasing Hamiltonian range. The DMM method therefore outperforms the FOE method under such circumstances (Daniels and Scuseria 1998). Hamiltonian matrices of relatively large range are found in the context of Density Functional calculations using Gaussian basis sets. For Tight Binding calculations, in contrast, the range of the Hamiltonian is usually small. The OM method shows the same behavior as the FOE method. The numerical effort increases linearly with respect to the number of nonzero elements per column of the Hamiltonian. In the DC method the numerical effort is independent of the bandwidth, but it is not expected that even in this case the DC method might outperform the FOE or DMM method.

- Scaling with respect to the size of the basis set:

Let us now consider the case, where the number of atoms as well as all other relevant quantities, such as the size of the localization region, are fixed and where we only increase the number of basis functions per atom m_b . Both the size and the number of off-diagonal elements per column of the density matrix will then increase. We will also assume that the Hamiltonian is a sparse matrix with m_b off diagonal elements per column. In the DMM method the numerical effort will consequently grow cubically with respect to m_b , since the number of operations needed for the multiplication of two sparse matrices of size n with m off-diagonal elements per column is proportional to $n m^2$. The DC method scales cubically as well since it is based on diagonalization. The FOE method equally scales cubically, since three factors are increasing. The number of columns in the density matrix, the number of coefficients in each column and the number of off-diagonal elements of the Hamilto-

nian matrix. In addition to the arguments showing the unrealistically large memory requirements of these methods when used with large basis sets, we thus also find a cubic scaling which prohibits the use of these algorithms in this context.

In the OM method both the application of the Hamiltonian to the orbitals as well as the calculation of the overlap between the orbitals scale quadratically with respect to m_b .

- Memory requirements:

The DMM method requires the storage of the whole sparse density matrix. If one takes advantage of the fact that the matrix is symmetric storage can actually be cut into half. The OM method requires only the storage of the truncated Wannier orbitals and so the memory requirements are reduced by about 50 percent in the typical Tight Binding context compared to the case where one stores all the nonzero elements of the density matrix without taking advantage of its symmetry. If the Kim formulation is used the gain can come down to less. In both the DC and FOE method only the subparts respectively the columns of the density matrix which are consecutively calculated need to be stored. The storage requirements are therefore greatly reduced compared to the DMM and OM methods, namely by a factor of roughly N_{el} .

- Parallel implementation:

Parallel computers and clusters of workstations are standard tools in the high performance computing environment. The suitability of an algorithm for parallelization is therefore also an important aspect. It is of course always possible to parallelize any program, the question is just whether this can be done in a coarse or fine grained way, i.e. with a small or large communication to computation ratio. Only a coarsened grained parallel program will run efficiently on clusters of workstations with relatively slow communications as well as on a very large number of processors of a massively parallel computer. Both the FOE and the DC algorithms are intrinsically parallel algorithms, meaning that the big computational problem is subdivided into smaller subproblems which can be solved practically independently. In the case of the FOE method (Goedecker and Hoisie 1997) the calculations of the different columns of the density matrix are practically independent (Equation (49)). In the case of the DC method the calculations of the different patches of the density matrix are practically independent as well. Both methods can therefore be implemented in a coarse grained way. A parallel program based on the FOE method won the 1993 Gordon Bell prize in parallel computing for its outstanding performance on a cluster of 8 workstations, obtaining half of the peak speed of the whole configuration (Goedecker and Colombo 1994). Impressive speedups of up to 400 have been obtained with the FOE method on a 800 processor parallel machine (Kress *et al.*, 1998). Even though it is more difficult to implement the OM method in parallel two such implementations have been reported. In the OM method two parallelization schemes are conceivable. In the first scheme (Canning *et al.*, 1996) one associates to each processor a certain number of localized orbitals. This data structure is optimal for the application of the Hamiltonian to the orbitals, but requires communication

for the calculation of the overlap between the orbitals. The second scheme (Itoh *et al.*, 1995) associates the coefficients of all the orbitals whose localization region has an intersection with a certain region of space to a certain processor. This data layout is optimal for the calculation of the overlap matrix, but requires communication for the application of the Hamiltonian. The OBDMM method has also been parallelized (Goringe *et al.*, 1997b). Since the OBDMM is more complex than the other methods that have been implemented on parallel machines three different parallelization paradigms are required.

- Quality of forces:

In the case of the variational (DMM and OM) methods the force formula is particularly simple (Equation 90) since only the Hellman Feynman term survives. It has to be stressed that this formula is however only exact if one has succeeded in reducing the gradient with respect to all variational quantities really to zero. If, in a simulation, the gradient is not reduced to zero within the required precision because too many iterations would be required, errors will creep into the calculated forces, making them inconsistent with the total energy. From this point of view the situation is easier in the FOE method. Since the FOE method is not an iterative method (in the sense that one iterates until a certain accuracy criterion is met), the force formula of Voter (Equation (58)) will always give forces consistent with the total energy. As has already been discussed no consistent force formula exists for the DC method.

Consistent forces are a prerequisite for the conservation of the total energy in Molecular Dynamics simulations. Even with consistent forces there are however other factors which can cause deviations from perfect total energy conservation in Molecular Dynamics simulations such as finite time steps and events where atoms enter or leave the localization region.

- Cases where the methods become inefficient:

Cases where different methods become inefficient have already implicitly been pointed out when discussing the previous criteria. Let us finally mention a special case where the FOE method is inefficient. As discussed above a small gap implies usually highly extended density matrices and the FOE method is highly competitive. There can however be exceptions to this rule. If by symmetry restrictions there is practically no coupling between two well localized states, which are close together, their energy levels can be split by a very small amount. If the Fermi level falls in between these two levels a very high degree polynomial is needed to separate these two levels in an occupied and an unoccupied one. This scenario can be found in the case of a vacancy in the silicon crystal. A Jahn Teller distortion leads to a very small splitting between an occupied and an unoccupied gap level. Using a high electronic temperature and a low degree polynomial in the FOE method does not reproduce this Jahn Teller distortion. A detailed study of this effect is given by Voter *et al.*, (1996) showing that a polynomial of degree 200 is needed instead of the typical polynomial of degree 50 needed for bulk silicon in the Tight Binding context. From an energetic point of view it is frequently not necessary to track such Jahn Teller

distortions, since they lead to a rather small energy lowering. In molecular dynamics simulations of metallic systems this suppression of the opening of a gap can even be beneficial (Goedecker and Teter 1995) since it leads to a smoother density of states around the Fermi level.

In summary, we see that the performance depends critically on many parameters which can change from one application to another. Performance superiority claims based on test runs of a particular system have therefore to be taken with caution.

4.2 Large basis sets

Whereas the methods which are mainly applicable in the context of small basis sets showed important differences under the various comparison criteria, the behavior of the FOP, OM and OBDMM methods are quite similar under most of these criteria. The comparison of the methods which are applicable to large basis sets will therefore be based only on a smaller set of important criteria.

- Scaling with respect to the size of the basis set:

As pointed out before the methods compared in this sections all have a reasonable scaling with respect to the size of the basis set allowing thus their use in the context of very large basis sets. In contrast to the discussion of the same point within the small basis set framework, the number of nonzero matrix elements of the Hamiltonian is typically independent of the resolution of the grid, i.e. of the number of basis functions. The most important part of the FOP, OM and OBDMM algorithms, the application of the Hamiltonian matrix to a wave vector scales therefore linearly. At the same time all these algorithms require at some stage the calculation of an overlap matrix among the occupied orbitals. This part scales quadratically as discussed before.

- Finding a first initial guess:

As discussed in the comparison part dealing with small basis sets, it can be difficult to find an initial guess for Wannier function based methods. This problem does not exist in the OBDMM method if the number of orbitals is larger than the number of electrons. In this case the orbitals are just basis functions and by analogy with the usual tight binding or LCAO basis sets it should always be possible to generate a physically motivated initial guess for these orbitals.

- Required number of iterations:

As mentioned both the OM and OBDMM methods suffer from ill-conditioning problems and require therfore a frequently excessive number of iterations for the iterative minimization. No such ill-conditioning exists for the FOP method.

- Cases where the methods become highly inefficient:

None of the 3 methods have ever been applied to metallic systems, and they are all expected to fail in this case.

5 Other $O(N)$ methods

The recursion method is a well established method which also exhibits $O(N)$ scaling. It is principally a method to calculate the density of states $D(\epsilon)$, but once the density of states is known, the band structure energy can be calculated by integrating $\epsilon D(\epsilon)$ up to the Fermi level. The recursion method has been described extensively (Haydock 1980, Gibson *et al.*, 1993) and we will therefore not review it. Let us just point out that within the original formulation of the recursion method only the diagonal elements of the density matrix could be calculated. For the calculation of the forces one would however also need the off-diagonal elements. So the applicability of the recursion method is significantly reduced compared to the $O(N)$ method described in section 3, which all gave access to the forces. There have been several attempts to overcome this limitation (Aoki 1993, Horsfield *et al.*, 1996b, Horsfield *et al.*, 1996c, Bowler *et al.*, 1997). In contrast to the methods of section 3 these Bond Order Potential (BOP) methods are fairly complex and difficult to implement. The basic idea in the BOP method is to calculate the off diagonal elements of the density matrix as the derivative of diagonal elements of a density matrix defined with respect to a transformed basis. Even though it is now possible to calculate forces within the BOP method, they are unfortunately not consistent with the total energy. In another version of the recursion method the GDOS method (Horsfield *et al.*, 1996b, Horsfield *et al.*, 1996c) the exact forces can be calculated. It is however necessary to calculate some generalized moments H^k called interference terms from the recursion coefficients. This inversion is ill conditioned and becomes unstable if one tries to calculate more than 20 moments (Bowler *et al.*, 1997). With such a low number of moments it is however not possible to describe many realistic systems (Kress and Voter 1995) and the error one reaches when the instability sets in is frequently still much too large to be acceptable (Bowler *et al.*, 1997). So recursion based methods seem not to be a general purpose tool for electronic structure calculations where accurate energies and forces are required. BOP methods can however give insight into basic bonding properties of crystalline solids (Pettifor). Since in these methods related to the recursion algorithm all the diagonal elements of the density matrix have to be calculated, they are obviously not very efficient if a very large number of basis functions per atom is used and they were indeed primarily proposed for Tight Binding or other schemes with a small number of basis function. The only exception is a version proposed by Baroni *et al.* (Baroni and Giannozzi 1995) who suggest to use delta functions as a basis in a Density Functional type calculation. With his basis set the diagonal elements of the density matrix are enough to determine the charge density, whereas for more general basis functions the off diagonal elements are needed as well (Equation (12)). Because the number of delta functions has to be very large even in the most favorable case of silicon, the crossover point was estimated to be around 1000 silicon atoms. This method is therefore clearly not competitive with most other methods where the cross over point is much lower.

Another approach to improve the scaling properties is based on so called pseudo-diagonalization (Stewart *et al.*, 1982). The method is closely related to the well known Jacobi method for matrix diagonalization. Whereas in the original Jacobi method rotation transformations are applied until all off-diagonal elements vanish, only the entries which couple occupied and unoccupied states are annihilated in the pseudo-diagonalization

method. One obtains thus not the occupied eigenvectors of the Hamiltonian but an arbitrary set of vectors which span the same occupied space. In its original formulation (Stewart and Pulay 1982) this method still had cubic scaling however with a smaller prefactor than complete matrix diagonalization. Nearly linear scaling has been reported with this method (Stewart 1996) if the Hamiltonian matrix is constructed with respect to a set of well localized orbitals. In this way most of the elements in the block coupling occupied and unoccupied states are zero at the start of the transformations. The annihilation of certain matrix elements during the rotation steps causes only a controlled spread of other rows and columns in the matrix. So at the end each column and row extends over a region which is comparable to the localization region in other $O(N)$ methods.

A method proposed by Galli and Parrinello (1992) can be considered as a predecessor of the OM method. The total energy is minimized with respect to a set of localized Wannier functions. In contrast to the OM method one has however the old conventional functional (Equation (93)) which has to be minimized under the constraint of orthogonality, whereas in the OM method the orthogonalization constraint is contained in the modified functional (Equation (92)). In this scheme it is necessary to calculate the inverse of the overlap matrix between the Wannier functions. From timing considerations this is not a serious drawback since this part is only a small fraction of the total workload even for large systems and even if it is done with a scheme which scales cubically. There are, however, problems of numerical stability. As pointed out by Pandey *et al.* (1995) the overlap matrix becomes close to singular and the introduction of localization constraints can under these circumstances falsify the results.

Also vaguely related to the OM functional are methods where certain constraints are included by a penalty function. Wang and Teter (1992) included the orthogonality constraint in this way, Kohn (1996) the idempotency condition of the zero temperature density matrix.

$O(N)$ implementations of electronic structure methods based on the multiple scattering theory have also been reported. In the simplest version (Wang *et al.*, 1995) it is essentially a DC method with the difference that within each localization region the calculation is done with the multiple scattering method. A further development was to replace the buffer region by an effective medium (Abrikosov *et al.*, 1995, Abrikosov *et al.*, 1996). This can considerably reduce the prefactor of the calculation, especially in metallic systems where large localization regions are needed. For this class of methods no force formulas have however been reported, a deficiency restricting their applicability.

A scheme which possibly leads to a reduced scaling behavior has also be proposed by Alavi *et al.*, (1994) It is based on a direct representation under the form of a sparse matrix of the Mermin finite temperature functional (Mermin 1965). So it allows for a finite temperature as does the FOE method.

As was already mentioned the polynomial FOE method becomes inefficient in cases where one has a large basis set causing the highest eigenvalue to grow very large. This would necessitate a Chebychev polynomial of very high degree. A elegant method to overcome this bottleneck within a polynomial method has been proposed by Baer and Head-Gordon (1998). They write the density matrix at a low temperature T as a telescopic

expansion of differences of density matrices at higher temperatures Tq^j .

$$F_T = F_{Tq^n} + (F_{Tq^{n-1}} - F_{Tq^n}) + (F_{Tq^{n-2}} - F_{Tq^{n-1}}) + \dots + (F_{Tq^0} - F_{Tq^1}) \quad (101)$$

The factor q determining the geometric sequence of temperatures is chosen from considerations of numerical convenience. As the temperature is lowered the numerical rank of each difference term becomes smaller and smaller since the difference of two Fermi distributions of similar temperature is vanishing to within numerical precision over most of the spectrum. Hence it is necessary to find Chebychev expansions only over successively smaller regions of the spectrum and it is also possible to calculate the traces (which in turn determine all physically relevant quantities) within spaces of smaller and smaller dimension.

Ordejon *et al.* (1995) proposed a method based on the OM method to calculate phonons from the electronic structure with linear scaling.

This article concentrated on O(N) methods which are able to calculate the total energy of a system as well as its derived quantities such as the forces acting on the atoms. Let us finally still point out that there are also several O(N) methods which primarily calculate the density of states and thus give information about the eigenvalue spectrum of a system. These methods (Drabold and Sankey 1993, Wang 1994, Silver and Roeder 1997) are not described in this article. In principle, it would also be possible to derive band structure and total energies from the spectrum by an integration up to the chemical potential. Attempts in this direction have however not been very successful up to now with the exception of the smeared density of states Kernel Polynomial method (Voter *et al.*, 1996) which is closely related to the FOE method.

6 Some further aspects of O(N) methods

Hierse and Stechel (1994, 1996) examined whether non-orthogonal Wannier like orbitals are transferable from one chemical environment to another similar one. If this was the case one could reuse precalculated Wannier orbitals as a very good initial starting guess. Such a property would thus reduce the prefactor of any method regardless of its scaling behavior. Unfortunately, they could find reasonable transferability only under rather restrictive conditions. When they added CH_2 units to a C_nH_{2n+2} polymer they found good transferability of the orbitals associated with this building block within a Density Functional scheme (Hierse and Stechel 1994). As soon as they started bending the polymer (Hierse and Stechel 1996), the transferability was however lost in the Density Functional scheme. Only in a non-self-consistent Harris functional scheme some efficiency gains were still possible.

Hernandez *et al.* (1997) suggest a solution to the basis set problem in O(N) methods. As was mentioned in section 3 O(N) techniques are difficult to reconcile with extended basis sets such as plane waves. Plane waves have however several important advantages and are therefore widely used in conventional (i.e. not O(N)) electronic structure calculations. One of their main advantages is that the accuracy can easily be improved by increasing one single parameter, namely the minimal wavelength which corresponds to the resolution in real space. Hernandez *et al.* proposed now a basis set of “blip” functions

which combines both advantages. It is localized and its resolution can systematically be improved. As an alternative to the “blip” functions one could also use finite difference techniques (Chelikowsky *et al.*, 1994) or wavelets (Lippert *et al.*, 1998, Goedecker and Ivanov 1998b, Arias 1998, Goedecker 1998b) since they share the same advantages. As shown by Goedecker and Ivanov (1998c) wavelets allow for highly compact representation of both the density matrix and the Wannier functions, since they are localized both in real and Fourier space.

Much of the work of Ordejon (1996) is also based on a new set of basis functions proposed by Sankey and Niklewski (1989). This basis set consists of atomic orbitals which are modified in such a way that they are strictly zero outside a certain spherical support region. This then gives rise to a Hamiltonian matrix which is strictly sparse. By tabulating these matrix elements it is possible to do Density Functional calculations whose computational requirements are in between the requirements of traditional Density Functional calculations and Tight Binding calculations. Obviously one has to find a compromise between accuracy and speed. If the basis functions extend about a larger support region, one has a more accurate basis, but the the numerical effort increases because the Hamiltonian is less sparse.

Horsfield and Bratkovsky (1996d) have incorporated entropy terms in $O(N)$ methods within the FOE algorithm. As soon as one has systems at nonzero temperature, these terms should in principle be added, however in most systems their effects are very small at room temperature. For computational convenience temperatures much larger than room temperature can however be used. Wentzcovitch *et al.* (1992) and Weinert and Davenport (1992) showed that the inclusion of entropy gives simplified force formulas, since only the Hellmann-Feynman term survives. The free energy A is given by

$$A = \text{Tr}[F H - k_B T S(F)], \quad (102)$$

where the entropy S is a matrix function of F

$$S = -(F \ln(F) + (1 - F) \ln(1 - F)). \quad (103)$$

Writing S as a Chebychev polynomial in H and analyzing everything in terms of the eigenfunctions of H they find that one has to do a Chebychev fit to a distribution very similar to the Fermi distribution just with some additional features close to the chemical potential. Using a formalism by Gillan (1998) they then extrapolate their results to zero temperature obtaining faster convergence to the zero temperature limit in this way. Let us stress again, that with the FOE method it is possible to build up density matrices corresponding to several temperatures without significant extra cost. A set of generalized Fermi distributions which allow an efficient extrapolation to the zero temperature limit by eliminating arbitrarily high powers of T has also been proposed by Methfessel and Paxton (1989)

As was mentioned in the introduction the fundamental cubic term in an electronic structure calculation based on orbitals comes from the orthogonalization requirement. In traditional pseudopotential calculations based on a Fourier space formulation there is however a second very large cubic term, arising from the nonlocal part of the pseudopotential. This second cubic term can be eliminated by using pseudopotentials which are

separable in real space (King-Smith *et al.*, 1991, Goedecker *et al.*, 1996, Hartwigsen *et al.*, 1998)

7 Non-orthogonal basis sets

Up to now we have always implicitly assumed that we are dealing with orthogonal basis sets, i.e. that

$$\int \phi_i^*(\mathbf{r}) \phi_j(\mathbf{r}) d\mathbf{r} = \delta_{i,j} . \quad (104)$$

Non-orthogonal basis sets give rise to an overlap matrix S ,

$$S_{i,j} = \int \phi_i^*(\mathbf{r}) \phi_j(\mathbf{r}) d\mathbf{r} . \quad (105)$$

An orthogonality relation similar to Equation (104) can be obtained by introducing the dual basis functions $\tilde{\phi}_i(\mathbf{r})$ given by

$$\tilde{\phi}_i(\mathbf{r}) = \sum_j S_{i,j}^{-1} \phi_j(\mathbf{r}) , \quad (106)$$

where S^{-1} is the inverse of the overlap matrix S . It is then easy to verify that

$$\int \tilde{\phi}_i^*(\mathbf{r}) \phi_j(\mathbf{r}) d\mathbf{r} = \delta_{i,j} . \quad (107)$$

As has been mentioned in section 3 all realistic atom centered localized basis sets are non-orthogonal. Within the Tight Binding context, there are also many non-orthogonal schemes on the market. There is thus certainly a need to apply O(N) techniques also for these schemes. Most of the basic O(N) algorithms presented previously have therefore been generalized to the non-orthogonal case and we will present these generalizations in the following. In the context of a non-orthogonal scheme one has to distinguish carefully between the eigenfunctions Ψ_n and the associated eigenvector \mathbf{c}^n which contain the expansion coefficients c_i^n such that $\Psi_n(\mathbf{r}) = \sum_i c_i^n \phi_i(\mathbf{r})$. The eigenvector \mathbf{c}^n satisfies the generalized eigenvalue equation

$$H\mathbf{c}^n = \epsilon_n S \mathbf{c}^n . \quad (108)$$

In the same way one has to distinguish carefully between the density matrix operator $F(\mathbf{r}, \mathbf{r}')$ and the density matrix $F_{i,j}$ itself. While the expression (22) for the density matrix operator remains the same,

$$F(\mathbf{r}, \mathbf{r}') = \sum_n f(\epsilon_n) \Psi_n^*(\mathbf{r}) \Psi_n(\mathbf{r}') = \sum_n f(\epsilon_n) \sum_{i,j} c_i^{n*} c_j^n \phi_i^*(\mathbf{r}) \phi_j(\mathbf{r}') \quad (109)$$

the expression for the number of electrons (Equation (13)) is modified to

$$N_{el} = Tr[F S] . \quad (110)$$

The expression for the band structure energy (10) however remains valid. In the definition of the density matrix $F_{i,j}$ (Equation (9)) one has to use now the dual basis functions instead of the ordinary,

$$F_{i,j} = \int \int \tilde{\phi}_i^*(\mathbf{r}) F(\mathbf{r}, \mathbf{r}') \tilde{\phi}_j(\mathbf{r}') d\mathbf{r} d\mathbf{r}' = \sum_n c_i^{n*} c_j^n f(\epsilon_n) \quad (111)$$

This replacement can have important consequences for the locality of the density matrix $F_{i,j}$. If we have a set of localized orthogonal basis functions (the only known set of basis functions with this property are the Daubechies scaling functions), whose extension is less than the oscillation period of the density matrix operator then Equation (9) ensures that $F_{i,j}$ will have the same decay properties as $F(\mathbf{r}, \mathbf{r}')$. This does not necessarily hold true for Equation (111). Even if the basis functions $\phi_i(\mathbf{r})$ are well localized this is in general not true for their duals $\tilde{\phi}_i(\mathbf{r})$. If the duals have a very slow decay then this slow decay will be inherited by $F_{i,j}$ and it might not be possible to use $O(N)$ algorithms for the calculation of $F_{i,j}$. Problems might for instance arise if high quality Gaussian basis sets containing diffuse functions are used. Preliminary experience indicates that for small basis sets of moderate quality the duals are not so delocalized as to destroy the localization of $F_{i,j}$.

In the case of the DC method the generalization to the non-orthogonal case is trivial. Since it is based on diagonalization within each subvolume one has to solve just the generalized eigenvalue problem (Equation (108)) instead of an ordinary one. In the Density Functional context, the DC method has actually only been used with non-orthogonal orbitals.

The FOE method using a Chebychev representation of the density matrix has been generalized by Stephan *et al.* (1998). It is easy to see that all the central equations of the FOE method remain correct if the Hamiltonian H is replaced by a modified Hamiltonian \bar{H} (that is not any more hermitian) given by

$$\bar{H} = S^{-1}H. \quad (112)$$

In particular, it remains true that the density matrix is given within arbitrary precision by

$$F \approx \frac{c_0}{2}I + \sum_{j=1}^{n_{pl}} c_j T_j(\bar{H}) \quad (113)$$

if a sufficiently large n_{pl} is used. The problem is how to find \bar{H} efficiently. Even if S is a sparse matrix the inverse S^{-1} is not sparse in general and \bar{H} would be a full matrix as well, destroying immediately the linear scaling. However, it turns out that the matrix elements of \bar{H} decay faster than the corresponding matrix elements of H (Stephan 1998, Gibson 1993). One can therefore cut off the Tight Binding Hamiltonian \bar{H} at the same distance where one would usually cut off H . In this way all the matrices involved are reduced to sparse matrices and \bar{H} can be constructed by solving the set of linear systems

$$S\bar{H} = H. \quad (114)$$

Since both the right hand sides in H and the solution vectors making up \bar{H} are sparse different systems of equations are only coupled by subblocks of S . So the big matrix inversion problem is decoupled into many small systems of equations and the scaling is therefore strictly linear.

If the FOP method is used in connection with a rational approximation the generalization to the non-orthogonal case can be done straightforwardly and without any approximation (Goedecker 1995)

$$F = \sum_{\nu} \frac{w_{\nu}}{H - z_{\nu}S}. \quad (115)$$

One has then to solve a systems of linear equations which is a generalization of Equation (73)

$$(H - z_\nu S)F_\nu = I \quad (116)$$

$$F = \sum_\nu w_\nu F_\nu. \quad (117)$$

A similar approach was adopted by Jayanthis *et al.* (1998). They formulated their method in terms of the Green function. However, F_ν in Equation (116) is a Green function for a complex energy z_ν and the methods are essentially equivalent.

If the FOE method is used to calculate Wannier functions the required projection operator F_p is slightly different from the density matrix and it is given by

$$F_p = \sum_\nu \frac{w_\nu S}{H - z_\nu S}. \quad (118)$$

The DMM method has also been generalized to the non-orthogonal case (Nunes and Vanderbilt 1994). Introducing a modified density matrix \bar{F} defined as

$$\bar{F} = S^{-1}FS^{-1} \quad (119)$$

the DMM functional (78) becomes

$$\Omega = \text{Tr}[(3\bar{F}S\bar{F} - 2\bar{F}S\bar{F}S\bar{F})(H - \mu I)]. \quad (120)$$

This has the advantage that one does not have to invert S if one minimizes directly with respect to \bar{F} . The calculation of the gradient of the DMM functional in the non-orthogonal case is a tricky point. The definition of the gradient is not as absolute as one might think. It is the direction of steepest descent per unit change of the variables, and one must therefore define a norm for the multidimensional space of variables before defining the gradient (D. Vanderbilt private communication). Two different gradient expression have been proposed by Nunes and Vanderbilt (1994) and by White *et al.* (1997) which correspond to two different choices of metric. The gradient of White *et al.* (1997) requires less minimization steps (Gillan *et al.*, 1998), but each minimization step is more expensive since it requires the calculation of the inverse of the overlap matrix. From the point of view of overall numerical efficiency it is therefore not clear which gradient expression is more efficient.

Another generalization (Millam and Scuseria 1997, Daniels *et al.*, 1997) of the DMM method which is similar in spirit to Stephan's generalization of the FOE method consists in first performing a transformation to an orthogonal basis set by finding the LU decomposition of the overlap matrix

$$S = U^T U, \quad (121)$$

where U is an upper triangular matrix. If in addition U is approximated as a sparse matrix with m off-diagonal elements then Equation (121) can be solved with a scaling proportional to $n m^2$ where n is the dimension of the matrices involved. Thus the scaling with respect to the size of the system is linear as it should be.

The OM method can easily be generalized to the non-orthogonal case (Ordejon *et al.*, 1996). The orbital overlap $\sum_l c_l^n c_l^m$ in the OM functional (Equation (92)) has to be generalized to $\sum_{l,k} c_l^n S_{l,k} c_k^m$.

8 The calculation of the selfconsistent potential

We will now discuss an issue which is relevant only in selfconsistent electronic structure calculations, namely the calculation of the potential arising from the electronic charge. This potential consists essentially of two parts, the electrostatic or Hartree potential and the exchange correlation potential.

8.1 The electrostatic potential

The solution of Poisson's equation to find the electrostatic potential arising from a charge distribution ρ is a basic problem found in many branches of physics. Solution techniques are described in a wide variety of books and articles. We will therefore only point out a few aspects which are important in the special context of O(N) electronic structure calculations.

If one is dealing with an electronic charge density which has only one length scale Poisson's equation can be solved efficiently and with a scaling which is close to linear. Charge densities of this type are encountered in the context of pseudopotential calculations where one has eliminated the core electrons and where the characteristic length scale is the typical extension of an atomic valence electron. One can, for instance, use plane wave or multigrid techniques (Briggs) which both have a scaling proportional to $n \log(n)$ where n is the number of grid points.

The situation becomes problematic when core electrons are included. In this case one could in principle still use the above mentioned techniques with a increased resolution. One would still have linear scaling, but the prefactor would be so large to make it completely impractical both from timing and memory considerations. Exactly the same arguments apply to the representation of the wave functions themselves and for this reason ordinary plane waves are not used for all electron calculations.

A widely used basis set for all electron calculations are Gaussian type basis sets (Boys 1960). By varying the width of the Gaussians one can describe both core and valence electrons. The popularity of Gaussian type basis functions comes from the fact that many important operations can be done analytically (S. Obara and Saika, 1986) One property which we will use is that the product of two Gaussians is again a Gaussian centered in between the two original Gaussian type functions. The matrix elements of the electrostatic potential part of the Hamiltonian with respect to a set of Gaussian orbitals $g_i(\mathbf{r})$, $i = 1, \dots, M_b$ are given by

$$H_{i,j} = \int d\mathbf{r} g_i(\mathbf{r}) \left(\int d\mathbf{r}' \sum_{k,l} \frac{F_{k,l} g_k(\mathbf{r}') g_l(\mathbf{r}')}{|\mathbf{r} - \mathbf{r}'|} \right) g_j(\mathbf{r}) . \quad (122)$$

The elementary integral

$$\int d\mathbf{r} \int d\mathbf{r}' \frac{g_i(\mathbf{r}) g_j(\mathbf{r}) g_k(\mathbf{r}') g_l(\mathbf{r}')}{|\mathbf{r} - \mathbf{r}'|} \quad (123)$$

can also be calculated analytically (S. Obara and Saika, 1986). A straightforward evaluation of Equation (122) would then result in a quartic scaling. There are, however, many

well known techniques (Challacombe *et al.*, 1995) to reduce this scaling. The most obvious trick starts from the observation that there is a negligible contribution to the charge density ρ if the Gaussians g_l and g_k are centered far apart. Consequently the charge density is not a sum over M_b^2 product Gaussians G_m , ($G_m = g_l g_k$), but only over M_a such Gaussians

$$\rho(\mathbf{r}') = \sum_{k=1}^{M_b} \sum_{l=1}^{M_b} F_{k,l} g_k(\mathbf{r}') g_l(\mathbf{r}') \approx \sum_{m=1}^{M_a} c_m G_m(\mathbf{r}'). \quad (124)$$

The size of the auxiliary basis set M_a is proportional to M_b with a large prefactor which depends on the ratio of the largest to the smallest extension of the Gaussians as well as on the accuracy target. In a similar way matrix elements $H_{i,j}$ become negligible if the basis functions g_i and g_j are centered very far apart. Using these two approximations one obtains a quadratic scheme with a very big prefactor. An approximate quadratic scaling is also found in numerical tests (Strout and Scuseria 1995).

Another widely used method consists in fitting the charge density by a set of M_a auxiliary Gaussians G_i . Even though we use the same symbols (M_a , G_i) as above they denote now somewhat different quantities. The allowed number of auxiliary Gaussians M_a is now much smaller, namely a few times M_b . The auxiliary functions themselves are therefore not anymore taken to be all the possible product functions, but determined by empirical rules in such a way as to give the best possible fit in Equation (124). The fitting involves the solution of an ill conditioned system of linear equations and has therefore cubic scaling, however with a small prefactor. The evaluation of the matrix elements using this representation of the charge density has then quadratic scaling if one again neglects small elements.

To obtain an even better scaling behavior requires the introduction of completely new concepts. One possibility is to build upon algorithms which solve the classical Coulomb problem for point particles. The classical Coulomb problem requires the calculation of the electrostatic potential arising from all the N particles with charge Z_j at all the positions \mathbf{r}_i

$$U(\mathbf{r}_i) = \sum_j \frac{Z_j}{|\mathbf{r}_i - \mathbf{r}_j|}. \quad (125)$$

By grouping particles into hierarchical groups and by describing their potential far away from such groups in an controlled approximate way by multipoles these fast algorithms allow to evaluate Equation (125) with linear scaling instead of the expected quadratic one. There are now several proposals (Strain *et al.*, 1996, White *et al.*, 1994, Perez-Jorda 1997), how one can modify one of these fast algorithms, the Fast Multipole Method (Greengard 1994) in such a way that it can handle also the continuous charge distributions arising in the context of electronic structure calculations. The basic idea is fairly straightforward. As we saw the charge distributions is always given as a weighted sum of auxiliary Gaussians (Equation (124)). Now the electrostatic potential of such a Gaussian particle looks the same from a distance as the potential of a point particle. Concerning the far field, one can thus essentially take over the existing algorithms. To account for the non point like nature of the Gaussian particles one has however to correct the near field. Since the calculation of these local corrections have linear scaling the whole procedure has linear scaling as well. There are two problems with this kind of approach. First, one has only

linear scaling with respect to the size of the basis set if the volume covered by the basis set grows at least as fast as the size of the basis set. If one adds for example basis functions for a molecule of fixed size, to improve the accuracy of the basis set one does not any more have linear scaling. This is related to the fact that one can apply the fast far field treatment now to a smaller number of Gaussian particle interactions. This behavior can be easily understood by considering the extreme case where all Gaussian particles are centered very close together within a radius which is smaller than their width. In this case one evidently cannot use any more any far field techniques. The second problem is closely akin to the first. If one adds extended Gaussians to the system the efficiency deteriorates.

A method which scales strictly linear with respect to the size of the basis set, independently of whether the volume is increased at the same time or not and which can be applied within the context of any basis set, is based on wavelets (Goedecker and Ivanov 1998a). As the input to this method the charge density is needed on a real space grid which can have varying resolution. Thus near the core region of the atoms in a molecule the resolution can be arbitrarily increased. Using interpolating wavelets this charge density can uniquely be mapped to a wavelet expansion, since a wavelet expansion can compactly describe nonuniform functions. In the wavelet basis one can then iteratively solve Poissons equation

$$\nabla^2 V = -4\pi\rho. \quad (126)$$

The matrix representing the Laplace operator ∇^2 is sparse and the matrix times vector multiplications needed for the iterative solution of Equation (126) scale linearly. Using a preconditioning scheme in a basis of lifted wavelets the condition number is independent of the size and of the maximal resolution of the wavelet expansion and the number of iterations is therefore constant. Thus one obtains an overall linear scaling.

8.2 The exchange correlation potential

Within the most popular versions of Density Functional theory the exchange correlation potential is a purely local function. In the case of the Local Density Approximation (Parr and Yang) the exchange correlation potential at a certain point depends only on the density at that point, in the case of Generalized Gradient Approximations (Perdew *et al.*, 1996, Becke 1988, Lee *et al.*, 1988) it depends in addition still on the gradient of the density at that point. If one uses real space methods such as finite differences or finite elements as well as plane wave methods where the calculation of the exchange correlation potential is done on a real space grid as well, it is obvious that the numerical effort is linear with respect to the system size. If one uses more extended basis functions such as Gaussian type orbitals it becomes more difficult to achieve linear scaling (Stratmann *et al.*, 1996).

In the case of Hartree Fock calculations the exchange energy

$$\sum_{i,j} \int \int d\mathbf{r} d\mathbf{r}' \frac{\Psi_i(\mathbf{r}) \Psi_j(\mathbf{r}) \Psi_i(\mathbf{r}') \Psi_j(\mathbf{r}')}{|\mathbf{r} - \mathbf{r}'|} \quad (127)$$

seems to be as nonlocal as the Coulomb potential. Using Equation (23) one can however

rewrite the expression (127) to obtain

$$\int \int d\mathbf{r} d\mathbf{r}' \frac{F(\mathbf{r}, \mathbf{r}') F(\mathbf{r}, \mathbf{r}')}{|\mathbf{r} - \mathbf{r}'|} \quad (128)$$

showing that the exchange energy in an insulator is indeed a local quantity whose locality is determined by the decay properties of the density matrix. A linear method to evaluate exchange terms within Gaussian type electronic structure calculations based on the aforementioned locality properties has been devised by Schwegler and Challacombe (1996). An alternative method based on the Fast Multipole Method has been developed by Burant *et al.*, (1996).

9 Obtaining self-consistency

To do a self-consistent electronic structure calculation, two ingredients have to be blended. The first is the calculation of the density matrix in a fixed external potential, a topic which is the main focus of this article. The second is the calculation of the potential from a given electronic charge density which was discussed in the preceeding section (8.1). Even if both of these basic parts exhibit linear scaling, it is however not yet granted, that one has overall linear scaling. It might happen that the number of times one has to repeat these two basic parts increases with the size of the system.

The easiest scheme to combine the calculation of the density matrix and the calculation of the potential is the so called scalar mixing scheme. Given an input charge density ρ_{in} which determines the potential one obtains after the calculation of the density matrix for this potential via Equation (12) a new output density ρ_{out} . The new input density ρ_{in}^{new} is now not the output density ρ_{out} , but rather a linear combination of the old input density and the output density

$$\rho_{in}^{new}(\mathbf{r}) = \rho_{in}(\mathbf{r}) + \alpha(\rho_{out}(\mathbf{r}) - \rho_{in}(\mathbf{r})) . \quad (129)$$

Here α is the mixing parameter. Overall linear scaling is endangered if one has to decrease α for reasons of numerical stability as the system becomes bigger and if one consequently needs a larger number of iterations.

The standard theory of mixing (Dederichs and Zeller 1983, Ho *et al.*, 1982) is based on the dielectric response function in \mathbf{k} space. Within this theory numerical instabilities arise if the dielectric response functions tends to infinity as k tends to zero. This happens in a metal but not in an insulator where the dielectric response function always remains finite. Following the general philosophy of this paper to remain within a real space formalism, we will elucidate mixing under this perspective. The final conclusions are of course the same as the one based on the Fourier space theory.

Let us first consider a metal. We assume that we are doing a calculation for a one-dimensional metallic structure of length L . Let us also assume that due to deviations from the converged self-consistent charge density we transfer an incremental charge ΔQ_{in} from one end of the sample to the other. Using the basic formula for the potential in a capacitor we get a constant electric field in the sample giving rise to a potential difference of $\Delta U = L \Delta Q_{in}$ between the two ends. In a metal this potential difference will most

likely be larger than the HOMO LUMO separation (which vanishes for large systems) and we get a large charge transfer ΔQ_{out} . This charge transfer is related to the density of states at the Fermi level, $D(\mu)$, which in our one dimensional case is the number of states per length unit and per energy unit. So the total charge transfer ΔQ_{out} is given by

$$\Delta Q_{out} \approx D(\mu) L \Delta U = D(\mu) L^2 \Delta Q_{in} . \quad (130)$$

If this induced charge transfer ΔQ_{out} is larger than the initial transfer ΔQ_{in} then the charge transfer will exponentially increase in subsequent iterations and we have the numerical instability called “charge sloshing”. To avoid it the mixing factor α has to be proportional to $\frac{1}{D(\mu) L^2}$. Doing the same analysis in a three-dimensional structure all the lateral dimensions cancel and we get the same result concerning α . Denoting the volume of our sample by v we find that α is proportional to $v^{-2/3}$. So α has to be decreased with increasing volume and the number of iterations in the mixing schemes increases with increasing system size. Fortunately and contrary to the implications of Annett (1995), this charge sloshing can be eliminated by state-of-the-art techniques (Kresse, 1996). One possibility (Kerker 1981) is just to do the mixing in Fourier space and to have a k dependent mixing parameter $\alpha(k) = \alpha_0 \frac{k^2}{k^2 + k_0^2}$

$$\rho_{in}^{new}(\mathbf{k}) = \rho_{in}(\mathbf{k}) + \alpha_0 \frac{k^2}{k^2 + k_0^2} (\rho_{out}(\mathbf{k}) - \rho_{in}(\mathbf{k})) . \quad (131)$$

As we see long wavelength components (corresponding to small k values) are now strongly damped by

$$\alpha_0 k^2 = \alpha_0 \left(\frac{2\pi}{\lambda} \right)^2 \quad (132)$$

and the dampening has the correct dimensional behavior with respect to the wavelength λ which corresponds to the length L in our above dimensional analysis. Short wavelength contributions are just damped by α_0 and this constant dampening sets in when k becomes comparable in magnitude to k_0 . We know, that for wavelengths of the order of the interatomic spacing a mixing parameter somewhat smaller than 1 works well and so we can determine by these conditions the values of α_0 and k_0 .

Let us next examine whether we can have charge sloshing in an insulator. We will assume that the potential difference across the sample is not larger than the gap, in which case the discussion for the metallic case would rather apply. Again we consider a sample of length L . According to the modern theory of polarization in solids (King-Smith and Vanderbilt 1989) a polarization arises because the centers of the Wannier functions are displaced under the action of an electric field. Since the Wannier functions are exponentially localized, the charge which will build up at the two surfaces of our sample is mainly due to the displacements of the Wannier function in the elementary cells of the crystal right on the surface and the charge ΔQ_{out} is thus practically independent of the length of the sample. So the optimal mixing constant α is nearly independent of the size of the system and the number of iterations as well.

In conclusion, we see that linear scaling can also be obtained in the selfconsistent case and that even in a metal charge sloshing problems can be overcome.

Mixing is the natural choice if the DC or the FOE methods are used in a self-consistent calculation. If methods based on minimization (DMM and OM) are used one can alternatively also obtain the ground state by a single minimization loop (R. Car and M. Parrinello 1985, I. Štich *et al.*, 1989, M. P. Teter *et al.*, 1989, M. Payne, *et al.*, 1992) without distinguishing between density matrix optimization cycles and potential mixing cycles. As is not surprising after our discussion of mixing one finds (Annett 1995) that in an insulator the number of iterations does not depend upon whether one has a self-consistent type of calculation where the potential is varying during each minimization step or whether one has a fixed potential. In other words there is no charge sloshing. In metallic systems it is essential to have finite electronic temperature (Wentzcovitch *et al.*, 1992, Weinert and Davenport 1992, Kresse 1996) and therefore the minimization schemes cannot be applied straightforwardly in any case. Insofar Annett's analysis (Annett 1995) showing that in this case the scaling is at least proportional to $N_{at}^{4/3}$ is irrelevant.

A completely different approach to the mixing problem has recently been proposed by Gonze (1996). He calculates the gradient of the total energy with respect to the potential. His gradient expression does not depend on the wavefunctions and could thus well be combined with O(N) schemes.

10 Applications of O(N) methods

This chapter is not intended to be a comprehensive or even complete review of all the applications which were done using O(N) methods. It is rather intended as an illustration of the wide range of areas where O(N) methods allowed to study systems which were too big to be studied with conventional methods. In general one can say that most large-scale Tight Binding studies are nowadays done in the connection with O(N) methods. In those cases systems comprising from a few hundred up to many thousand atoms are typically studied. Treating such a large number of atoms with O(N) Density Functional methods is much more difficult. In the case of Density Functional calculations the benchmarking and verification aspect is usually dominating whereas in tight binding calculations the focus was in most cases on how to solve challenging physical problems.

Questions concerning extended defects in crystalline materials were one of the main focus of these Tight Binding studies. Because several good Tight Binding parameters are available for silicon, most studies were done for this material. The 90° partial dislocation in silicon was at the focus of interest of a series of tight binding studies. The three structures that were examined are shown in Figure 16.

The energy difference between the structure (a) and (b) of Figure 16 was studied both by Nunes *et al.* (1996) and by Hansen *et al.* (1995). Even though they used different TB parameters and different O(N) algorithms (DMM and FOE) the both obtained exactly the energy difference of .18eV/Å in favor of structure (b). Later Benetto and al. (1997) discovered a new structure (c) that is even lower in energy. To validate their tight binding results they did conventional density functional calculations for smaller subsystems finding perfect agreement with the O(N) tight binding results. This new structure is experimentally difficult to distinguish from structure (b) and so this result is a convincing illustration of the power of these new O(N) algorithms in materials science. All these

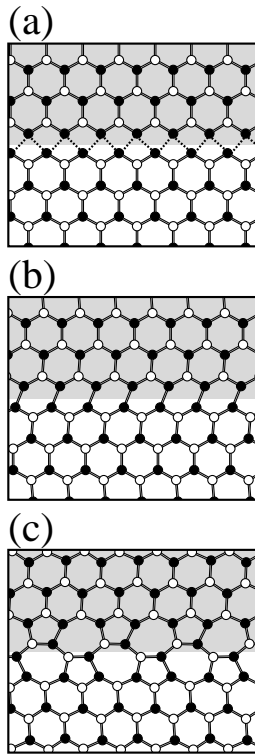


Figure 16: (a) *Symmetric reconstruction of the 90° partial dislocation in silicon. Shaded area indicates stacking fault.* (b) *the single-period symmetry breaking reconstruction.* (c) *The double-period symmetry breaking reconstruction.* The figure is reproduced with the kind permission of the authors from Nunes *et al.* (1998).

tight binding calculations necessitated electronic structure calculations involving a few hundred atoms and would therefore have been unfeasible with standard algorithms.

Extended {311} defects in silicon systems containing more than 1000 atoms and their relation to point defects were studied by Kim *et al.* (1997) using the OM method in the improved version of Kim *et al.* (1995). An understanding of these processes is important for the fabrication of semiconductor devices, since defects have a strong influence of the diffusion properties of semiconductors. Unfortunately, the more realistic questions involving boron dopant atoms in addition to the bulk silicon atoms can not be treated with current tight binding models.

Ismail-Beigi and Arias (1998) examined the surface reconstruction properties of silicon nanobars, finding that the influence of edges in these small structures is strong enough to lead to surface reconstructions that are different from the ones in bulk silicon. They also both employed traditional density functional calculations and $O(N)$ FOE tight binding calculations and also found good agreement between both for small subsystem which are accessible to both approaches.

Roberts and Clancy (1998) simulated vacancy and interstitial diffusion processes in silicon using the FOE tight binding method. The diffusion constants they obtain are in good agreement with similar calculations based on classical force fields and density

functional calculations. Compared to the density functional calculations they could also significantly enlarge both the number of atoms (216) and the simulation times. The diffusion constant predicted by all these simulations is however orders of magnitude larger than the experimental one, a fact for which no explanation is known up to now.

Besides silicon there is another material for which several good Tight Binding schemes are available, namely carbon. Fullerene systems are therefore another focus of Tight Binding studies.

Galli and Mauri (1994) did molecular crash test of C_{60} fullerenes colliding with a diamond surface using the OM method. They found three different impact energy regimes where the impinging fullerenes either survive the collision undamaged, slightly damaged or get completely destroyed. Even though the interaction region between the impinging fullerene and the surface does not comprise a very large number of atoms, their computational box contained more than 1000 atoms. The reason why the box has to be so large is that the phonons emitted during the collision may not be reflected back from the walls of the box during the time scale of the collision. This reflection of phonons is also a serious problem in classical force field simulations of crack propagation where for this reason systems comprising several million atoms are sometimes necessary (Zhou *et al.*, 1997). In the case of this molecular crash test most of the carbon atoms are propagating the phonons. Phonons are well described by classical force fields and one could use this scheme for the majority of the atoms, while it would be necessary to use the more expensive tight binding scheme only for the atoms in the collision region. Unfortunately such schemes combining molecular methods of different speed and accuracy have not yet been developed and thus it is therefore a feature of many $O(N)$ calculations that one is doing an overkill in a certain sense, treating a large number of essentially inactive atoms with highly accurate methods. Canning *et al.* (1997) examined thin films of C_{28} fullerenes with the same method, finding that thin superatom films can be formed.

The equilibrium geometries of large fullerenes such as C_{240} was also studied by several groups with $O(N)$ techniques. The central question here is whether such large fullerenes have a spherical form or a polyhedrally faceted shape, where nearly flat polyhedral regions are alternating with edges where the curvature is concentrated. York *et al.* (1994) used the original formulation of the DC method in terms of densities to do density functional calculations of C_{240} and found spherical shapes. Itoh and al. using both empirical and ab initio tight binding in the context of the OM method found however polyhedral shapes. This result is also supported by Xu and Scuseria (1996) who investigated fullerenes up to C_{8640} using the DM method. The optimized geometries they found for various large fullerenes are shown in Figure 17.

Ajayan *et al.* (1998) used tight binding FOE molecular dynamics to simulate irradiation mediated knock-out of carbon atoms out of carbon nanotubes. In agreement with experimental observations they found that this atom removal leads to a shrinking of the diameter of the nanotube, but leaves the nanotube essentially intact until the diameter is practically zero. They could identify in their virtual 400 atom sample processes on the atomic level that are responsible for the rapid healing of the defects created by the removal of atoms.

Recently developed Tight Binding parameters (Horsfield 1996a) made it possible to study also a composite system, namely hydrocarbons. This set of tight binding parameters

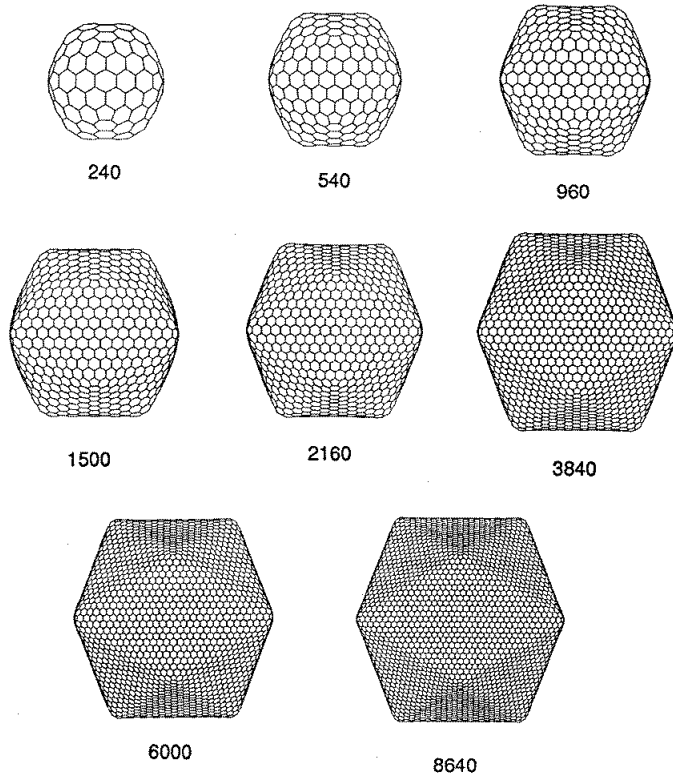


Figure 17: *Tight binding equilibrium geometries of selected icosahedral fullerenes viewed along the C_2 symmetry axis. This figure is reproduced with the kind permission of the authors from Xu and Scuseria (1996).*

includes some kind of self-consistency by imposing a local charge neutrality requirement. Local charge neutrality is essential if different phases are studied because it prevents any unphysically large charge transfer between different phases arising from different chemical potentials in different phases. Using this new tight binding scheme, Kress *et al.* (1998) studied the dissociation of CH_4 under high pressure and at high pressure using the FOE molecular dynamics. Previous Density functional based molecular dynamics studies by Ancilotto *et al.* (1997) were limited to very small system sizes of 16 CH_4 molecules and short simulation times of 2 ps. At variance with experimental findings these density functional simulations could not find a phase separation of methane into hydrogen and carbon. FOE molecular dynamics allowed to treat much larger systems of 128 molecules and also much longer simulation times of 8 ps. After 4 ps a phase separation was indeed observed.

Sanchez-Portal *et al.* (1997) compared the experimental X-ray structure of a large DNA molecule comprising 650 atoms with the geometric structure obtained from a density functional based OM relaxation. They obtained a root mean square deviation from the experimental geometry of 0.23 Å. Their method relies however on fairly drastic approximations resulting in errors that are by far larger than the error one generally expects from a density functional calculation.

A similar study of a large biomolecule is reported by Lewis *et al.* (1997).

York *et al.* used the DC method in the context of the semi-empirical AM1 method (Dewar *et al.*, 1985) to calculate heats of formation, solvation free energies and densities of states for protein and DNA systems containing up to 2700 atoms.

Daniels and Scuseria reported AM1 semi-empirical benchmark calculations for up to 20000 atoms using DMM, FOE and pseudo-diagonalization methods.

Applications of $O(N)$ methods within Density Functional theory, that use basis sets large enough such the basis set errors are not dominating the Density Functional error at present do not exist. If calculations of this type were done, such as the calculations of a cell containing 6000 silicon atoms by Goringe *et al.* (1997), then the performance evaluation aspect was always the dominating one. With the advance of faster computers and improved algorithms this situation will, however, certainly soon change. It is also interesting to note in this context that the 1998 version of the very popular Gaussian software package will contain $O(N)$ algorithms.

Let us finally come back to a point briefly mentioned in the introduction. The development of $O(N)$ methods has also deepened our understanding of locality in quantum mechanical systems and has thereby also fostered the development of theories based on a local picture rather than the conventional nonlocal Bloch function picture. An example is the theory of polarization in crystalline materials by King-Smith and Vanderbilt (1989). Their theory is based on a local picture in terms of Wannier functions and allows for an intuitive understanding of these phenomena that were difficult to understand before.

11 Conclusions

$O(N)$ methods have become an essential part of most large scale atomistic simulations based either on Tight Binding or semiempirical methods. The physical foundations of $O(N)$ methods are well understood. They are related to the decay properties of the density matrix. The use of $O(N)$ methods within Density Functional methods is still waiting for their widespread appearance. All the algorithms that would allow us to treat very large basis sets within density functional theory have certain shortcomings. The OM and OBDMM method suffer from ill-conditioning problems, and in both the OM and FOP method detailed knowledge about the bonding properties is required to form the input guess. Thus there is probably still some algorithmic progress necessary before these obstacles can be overcome. It is also not quite clear what the localization properties of very large complicated molecules are and whether perhaps a quadratic scaling rather than a linear scaling is the optimum one can obtain in certain cases. It is clear that the elimination of the cubic scaling bottleneck is a very important achievement and that it will pave the way for calculations of unprecedented size in the future. Such calculations will not only be beneficial to physics, but they will also nourish progress in many related fields such as chemistry, materials science and biology. Even with $O(N)$ algorithms it will not be possible in the foreseeable future to treat systems containing millions of atoms at a highly accurate Density functional level using large basis sets, as would be necessary for certain materials science applications. Such problems can only be approached if one succeeds in combining methods of different accuracy such as density functional methods with classical force fields, applying the high accuracy method only to regions where the

low accuracy method is expected to fail. Hybrid methods of this type will certainly be based on the same notions of locality and similar techniques as $O(N)$ methods.

12 Acknowledgments

I would like to express my deep gratitude to all the people who helped me to discover errors in the manuscript and who made valuable suggestions how to improve the paper. They are in alphabetical order David Bowler, David Drabold, Olle Gunnarson, Eduardo Hernandez, Andrew Horsfield, Jurg Hutter, Ove Jepsen, Joel Kress, Klaus Maschke, Richard Martin, Chris Mundy Ricardo Nunes, Michele Parrinello, Anna Puttrino, Gustavo Scuseria, Uwe Stephan, and David Vanderbilt .

13 Appendix: Decay properties of Fourier transforms

The density matrix is defined in terms of a Fourier transform given by Equation (26). The decay properties of the density matrix are thereby closely related to the decay properties of Fourier transforms. All the properties described in this paragraph are well known, for completeness we will briefly outline them.

For simplicity let us just consider a one-dimensional Fourier transform

$$g(r) = \int_{-\infty}^{\infty} e^{ikr} g(k) dk , \quad (133)$$

where $g(k)$ is an integrable piecewise continuous function tending rapidly to 0 for k tending to $\pm\infty$.

For any function $g(k)$ of this type, $g(r)$ will obviously tend to zero when r tends to infinity. In this case e^{ikr} is a very rapidly oscillating function and the product $e^{ikr} g(k)$ will therefore change sign very rapidly and thus the integral will tend to zero. The exact decay properties depend on how many derivatives are continuous. Let us consider first a function which is piecewise constant and has only a finite number of discontinuities. A function which falls into this class is the function $g(k)$ which is 1 in the interval [-1:1] and zero everywhere else. Calculating the Fourier transform one finds $g(r) = 2 \frac{\sin(r)}{r}$. Since any piecewise function $g(k)$ can be written as a linear combination of the above prototype function, its transform $g(r)$ will always decay like $1/r$. Using integration by parts we see that

$$r^l g(r) = \int_{-\infty}^{\infty} g(k) i^{-l} \left(\frac{\partial}{\partial k} \right)^l e^{ikr} dk = (-i)^{-l} \int_{-\infty}^{\infty} e^{ikr} \left(\frac{\partial}{\partial k} \right)^l g(k) dk . \quad (134)$$

If the l -th derivative is integrable then the integral will vanish for the reasons discussed above. So if we can do l integrations by parts each transformation will accelerate the decay by one inverse power of r and we can do such a transformation whenever our function has at least continuous first derivatives. Hence we arrive at the rule that if l derivatives of $g(k)$ are continuous, $g(r)$ will decay like $r^{-(l+1)}$.

If we have a function $g(k)$ which is analytic, i.e. one for which an infinite number of derivatives exists, then the transform will decay faster than any power of r . One then says that it decays exponentially instead of algebraically. This notion of exponential decay does not necessarily mean that it decays strictly like an exponential function. As an example we could for instance take $g(k) = \exp(-k^2)$, where we know that the transform is again a Gaussian and decays thus faster than an ordinary exponential function. The rate of decay will be related to the smallest length scale of $g(k)$. If the smallest length scale of $g(k)$ is k_{min} then $g(r)$ will roughly decay like $\exp(-c|r|k_{min})$, where c is a constant of order of 1. This follows from the fact that one will have an important cancellation of terms of opposite sign in the integral in Equation (133) only if several oscillations occur within the interval k_{min} .

Another qualitative feature of the Fourier transform is that it will have oscillations whenever $g(k)$ is shifted off center. The oscillation period is determined by this shift. As an example let us look at the Fourier transform of a shifted Gaussian $g(k) = \exp(-\frac{1}{2}(k-a)^2)$. The result is $g(r) = \sqrt{2\pi} \exp(iar) \exp(-\frac{1}{2}r^2)$, which is the transform of the unshifted Gaussian times an oscillatory term.

14 References

Abrikosov, I., A. Niklasson, S. Simak, B. Johansson, A. Ruban and H. Skriver, Phys. Rev. Lett. **76**, 4203 (1996)

Abrikosov, I., S. Simak, B. Johansson, A. Ruban and H. Skriver, Phys. Rev. B **56**, 9319 (1997)

Ajayan, P., V. Ravikumar and C. Charlier, Phys. Rev. Lett. **81**, 1437 (1998)

Alavi, A., J. Kohanoff, M. Parrinello and D. Frenkel, Phys. Rev. Lett. **73**, 2599 (1994)

Ancilotto, F., G. Chiarotti, S. Scandolo and E. Tosatti, Science **275**, 1288 (1997)

Annett, J., Comp. Mater. Science **4**, 23 (1995)

Aoki, M., Phys. Rev. Lett. **71**, 3842 (1993)

Arias, T., Rev. of Mod. Phys. ??, ?? (1998)

Ashcroft, N., and N. D. Mermin "Solid State Physics" Saunders College, Philadelphia, 1976

Ayala, P. and G. Scuseria, J. Chem. Phys., in press

Baer, R., and M. Head-Gordon, Phys. Rev. Lett. **79**, 3962 (1997)

Baer, R., and M. Head-Gordon, J. Phys. Chem. **107**, 10003 (1997)

Baer, R., and M. Head-Gordon, submitted to J. Phys. Chem.

Baroni, S., and P. Giannozzi, Europhys. Lett. **17**, 547 (1992)

Bates, K. R., A. D. Daniels, and G. E. Scuseria, J. Chem. Phys. **109**, 3308 (1998a).

Becke, A., Phys. Rev. A **38**, 3098 (1988)

Bennetto, J., R.W. Nunes, and David Vanderbilt, Phys. Rev. Lett. **79**, 245 (1997)

Blount, E., in "Solid State Physics" vol. 13, page 305, edited by F. Seitz and C. Turnbull, Academic Press, New York, 1962

Bowler, D., M. Aoki, C. Goringe, A. Horsfield and D. Pettifor, Modelling Simul. Mater. Sci. Eng. **5**, 199 (1997)

Bowler, D., M. Gillan, Comp. Phys. Comm. to be published (1998)

Boys, S., Proc. R. Soc. London, Ser. A **200**, 542 (1950)

Burant, J., G. Scuseria and M. Frisch, J. Phys. Chem. **105**, 8969 (1996)

Briggs, W., "A Multigrid Tutorial", SIAM, Philadelphia, 1987

Canning, A., G. Galli, F. Mauri, A. de Vita and R. Car, Comp. Phys. Comm. **94**, 89 (1996)

Canning, A., G. Galli and J. Kim, Phys. Rev. Lett. **78**, 4442 (1997)

Car, R., and M. Parrinello, Phys. Rev. Lett. **55**, 2471 (1985);

Challacombe, M., E. Schwegler and J. Almlöf, University of Minnesota Supercomputer Institut Research Report UMSI 95/186

Chalvet, O., Daudel, S. Diner, and J.-P. Malrieu (eds.), "Localization and Delocalization in Quantum Chemistry, vols. I - IV", Reidel, Dordrecht, 1976

Chelikowsky, J., N. Troullier and Y. Saad, Phys. Rev. Lett. **72**, 1240 (1994)

Cloizeaux, J. des, Phys. Rev. **135**, A685 and A698 (1964)

Daniels, A., J. Millam and G. E. Scuseria, J. Chem. Phys. **107**, 425 (1997)

Daniels, A., and G. E. Scuseria, J. Chem. Phys. (1998b), in press

Dederichs, P., and R. Zeller, Phys. Rev. B **28**, 5462 (1983)

Devar, M., E. Zoebisch. E. Healy and J. Stewart, J. Am. Chem. Soc. **107**, 3902 (1985)

Drabold, D., and O. Sankey, Phys. Rev. Lett. **70**, 3631 (1993)

Daw, M., Phys. Rev. B **47**, 10895 (1993)

Dickson, R., and A. Becke, J. Chem. Phys. **99**, 3898 (1993)

Erdelyi, A., editor, "Tables of Integral Transforms", McGraw-Hill, New York, 1954

Feynman, R., Phys. Rev. **56**, 340 (1939)

Fernandez, P., A. Dal Corso , A. Baldereschi and F. Mauri, Phys. Rev. B **55**, R1909 (1997)

Fulde, P. , "Electron Correlations in Molecules and Solids", Springer Series in Solid-State Sciences, Vol 100, 1995

Gagel, F., J. of Comp. Phys. **139**, 399 (1998)

Galli, G., and M. Parrinello, Phys. Rev. Lett. **69**, 3547 (1992)

Galli, G., and F. Mauri, Phys. Rev. Lett. **73**, 3471 (1994)

Galli, G., Current Opinion in Solid State and Materials Science **1**, 864 (1996)

Gibson, A., R. Haydock and J. P. LaFemina, Phys. Rev. B **47**, 9229 (1993)

Gillan, M., J. Phys. Condens. Matter, **1**, 689 (1989)

Gillan, M., D. Bowler, C .Goringe and E.Hernández, Proceedings of the Symposium on Complex Liquids, 10-12 November 1997, Nagoya, Japan, ed. T.Fujiwara and M.Doi (World Scientific, 1998)

Goedecker, S., Phys. Rev. B **48**, 17573 (1993)

Goedecker, S., L. Colombo, Phys. Rev. Lett. **73**, 122 (1994)

Goedecker, S., L. Colombo, Proc. Supercomputing 94, Washington D.C., November (1994)

Goedecker, S., M. Teter, Phys. Rev. B **51**, 9455 (1995)

Goedecker, S., J. of Comp. Phys. **118**, 261 (1995)

Goedecker, S., M. Teter, J. Hutter, Phys. Rev. B **54**, 1703 (1996)

Goedecker, S., and A. Hoisie, Los Alamos National laboratory, unclassified report, LA-UR-97-1504 (1997)

Goedecker, S., O. Ivanov, Sol. State Comm., **105**, 665 (1998a)

Goedecker, S., and I. Ivanov , Comp. in Phys. ??, ?? (1998b)

Goedecker, S., and I. Ivanov , Phys. Rev. B ??, ?? (1998c)

Goedecker, S., Phys. Rev. B **58**, 3501 (1998a)

Goedecker, S., "Wavelets and their application for the solution of differential equations", Presses Polytechniques Universitaires et Romandes, Lausanne, Switzerland (ISBN 2-88074-398-2), (1998b)

Gonze, X., Phys. Rev. B **54**, 4383 (1996)

Goodwin, L., J. Phys.: Condens. Matter **3**, 3869 (1991)

Goringe, C., D. Bowler and E. Hernandez, Rep. Prog. Phys. **60**, 1447 (1997a)

Goringe, C., E. Hernandez, M. Gillan and I. Bush, Comp. Phys. Comm. **102**, 1 (1997b)

Greengard, L., Science, **265**, 909 (1994)

Hammond, B.L., W.A. Lester and P.J. Reynolds, "Monte Carlo Methods in Ab Initio Quantum Chemistry", World Scientific 1994

Hansen, L., K. Stokbro, B. Lundquist, K. Jacobsen and D. Deaven, Phys. Rev. Lett., **75**, 4444 (1995)

Harrison, W., "Electronic Structure and the Properties of Solids" Dover, New York, 1980

Hartwigsen, C., S. Goedecker and J. Hutter, Phys. Rev. B **58**, 3641 (1998)

Haydock, R., Solid State Phys. **35**, 215 (1980)

Hehre, W. J., L. Radom, J. A. Pople and P. V. R. Schleyer, "Ab Initio Molecular Orbital Theory", John Wiley and Sons, New York, 1996.

Heine, V., Solid State Phys. **35**, 1 (1980)

Hernandez, E., and M. Gillan, Phys. Rev. B **51**, 10157 (1995)

Hernandez, E., M. Gillan, and C. Goringe, Phys. Rev. B **53**, 7147 (1996)

Hernandez, E., M. Gillan, and C. Goringe, Phys. Rev. B **55**, 13485 (1997)

Hierse, W., and E. Stechel, Phys. Rev. B **50**, 17811 (1994)

Hierse, W., and E. Stechel, Phys. Rev. B **54**, 16515 (1996)

Ho, K-M., J. Ihm and J. Joannopoulos, Phys. Rev. B **25**, 4260 (1982)

Horsfield, A., P. D. Godwin, D. G. Pettifor and A. P. Sutton, Phys. Rev. B **54**, 15773 (1996a)

Horsfield, A., A. Bratkovsky, D. Pettifor and M Aoki, Phys. Rev. B **53**, 1656 (1996b)

Horsfield, A., A. Bratkovsky, M. Fearn, D. Pettifor and M Aoki, Phys. Rev. B **53**, 12694 (1996c)

Horsfield, A., A. Bratkovsky, Phys. Rev. B **53**, 15381 (1996d)

Ismail-Beigi, S., and T. Arias, Phys. Rev. B **57**, 11923 (1998)

Itoh, S., P. Ordejon and R. M. Martin, Comp. Phys. Comm. **88**, 173 (1995)

Itoh, S., P. Ordejon, D. Drabold and R. Martin, Phys. Rev. B **53**, 1 (1996)

Jayanthi, C., S. Wu, J. Cocks, N. Luo, Z. Xie, M. Menon and G. Yang, Phys. Rev. B **57**, 3799 (1998)

Johnson, B., P. Gill and J. Pople. J. Chem. Phys. **98**, 5612 (1993)

Kerker, G., Phys. Rev. B **23**, 3082 (1981)

Kim, J., F. Mauri and G. Galli, Phys. Rev. B **52**, 1640 (1995)

Kim, J., and J. Wilkins, F. Khan and A. Canning, Phys. Rev. B **55**, 16186 (1997)

King-Smith, R., and D. Vanderbilt, Phys. Rev. B **47**, 1651 (1993)

King-Smith, R., M. Payne and J. Lin, Phys. Rev. B **44**, 13063 (1991)

Kittel, C., "Quantum Theory of Solids" John Wiley and Sons, New York, 1963

Kohn, W., Phys. Rev. **115**, 809 (1959)

Kohn, W., Phys. Rev. **133**, A 171 (1964)

Kohn, W., Phys. Rev. B **7**, 4388 (1973)

Kohn, W., Chem. Phys. Lett. **208**, (1993)

Kohn, W., Int. J. Quant. Chem. **56**, 229 (1995)

Kohn, W., Phys. Rev. Lett. **76**, 3168 (1996)

Kress, J., and A. Voter, Phys. Rev. B **52**, 8766 (1995)

Kress, J., S. Goedecker, A. Hoisie, H. Wassermann, O. Lubeck, L. Collins and B. Holian, Journal of Computer-Aided Materials Design, in press

Kresse, G., Phys. Rev. B **54**, 11169 (1996)

Landau, E. M. and L. P. Lifshitz, "Statistical Physics, Part 1", Third edition, Pergamon Press, New York, 1980

Lee, C., W. Yang and R. Parr, Phys. Rev. B **37**, 785 (1988)

Lewis, J., P. Ordejon and O. Sankey, Phys. Rev. B **55**, 6880 (1997)

Li, X.-P., W. Nunes and D. Vanderbilt, Phys. Rev. B **47**, 10891 (1993)

Lippert, R., T. Arias and A. Edelman, to appear in J. Comp. Physics

Majewski, J., and P. Vogl in “*The Structure of Binary Compounds*”, North Holland, Amsterdam (1989), p. 287

March, N., W. Young and S. Sampanthar, “*The Many-Body Problem in Quantum Mechanics*” Cambridge University Press, Cambridge, England, 1967

Marzari, N., and D. Vanderbilt, Phys. Rev. B **56**, 12847 (1997)

Maslen, P., C. Ochsenfeld, C. White, M. Lee and M. Head-Gordon, J. Phys. Chem. **102**, 2215 (1998)

Mauri, F., G. Galli and R. Car, Phys. Rev. B **47**, 9973 (1993)

Mauri, F., and G. Galli, Phys. Rev. B **50**, 4316 (1994)

McWeeny, R., Rev. Mod. Phys, **32**, 335 (1960)

McWeeny, R., “*Methods of Molecular Quantum Mechanics*”, Academic Press, New York 1989

Mermin, N., Phys. Rev. **137 A**, 1441 (1965)

Methfessel, M., and A. Paxton, Phys. Rev. B **40**, 3616 (1989)

Millam, J., and G. Scuseria, J. Chem. Phys. **106**, 5569 (1997)

Nicholson, D., and X.-G. Zhang, Phys. Rev. B **56**, 12805 (1997)

Nightingale, M. P. and C. J. Umrigar editors “*Quantum Monte Carlo Methods in Physics and Chemistry*”, NATO ASI Series, Series C, Mathematical and Physical Sciences, Vol. XXX, Kluwer Academic Publishers, 1998

Nunes, R., and D. Vanderbilt, Phys. Rev. B **50**, 17611 (1994)

Nunes, R., J. Bennetto, and David Vanderbilt, Phys. Rev. Lett. **77**, 1516 (1996)

Nunes, R., J. Bennetto, and David Vanderbilt, submitted to Physical Review B

Obara, S., and A. Saika, J. Chem. Phys. **84**, 3963 (1986)

Ordejon, P., D. Drabold, M. Grumbach and R. Martin, Phys. Rev. B **48**, 14646 (1993)

Ordejon, P., D. A. Drabold, R. M. Martin and M. P. Grumbach, Phys. Rev. B **51**, 1456 (1995)

Ordejon, P., E. Artacho and J. Soler, Phys. Rev. B **53**, R10441 (1996)

Pandey, K., A. Williams and J. Janak, Phys. Rev. B **52**, 14415 (1995)

Parr, R., and W. Yang, “*Density-Functional Theory of Atoms and Molecules*”, Oxford University Press, 1989

Payne, M., M. Teter, D. Allan, T. Arias and J. Joannopoulos, Rev. of Mod. Phys. **64**, 1045, (1992)

Perdew, J., K. Burke, and M. Ernzerhof, Phys. Rev. Lett. **77** 3865 (1996)

Perez-Jorda, J., and W. Yang, J. Chem. Phys. **107**, 1218 (1997)

Pettifor, D. “*Bonding and structure of molecules and solids*”, Clarendon Press, Oxford, 1995

Press, W., B. P. Flannery, S. A. Teukolsky and W. T. Vetterling, “*Numerical Recipes, The Art of Scientific Computing*” Cambridge University Press, Cambridge, England, 1986

Pulay, P., in “*Modern Theoretical Chemistry*”, H. F. Schaefer editor, Plenum Press, New York, 1977

Qui, S-Y., C. Wang, K. Ho and C. Chan, *J. Phys, Condens. Matter* **6**, 9153 (1994)

Roberts, B., and P. Clancy, submitted to *Phys. Rev. B*

Saad, Y., "Iterative methods for sparse linear systems" PWS Publishing Company, Boston 1996

Sankey, O., and D. Niklewski, *Phys. Rev. B* **40**, 3979 (1989)

Sankey, O., D. Drabold and A. Gibson, *Phys. Rev. B* **50**, 1376 (1994)

Schwegler, E., and M. Challacombe, *J. Chem. Phys.* **105**, 2726 (1996)

Silver, R., H. Roeder, A. Voter and J. Kress, *J. of Comp. Phys.* **124**, 115 (1996)

Silver, R., and H. Roeder, *Phys. Rev. E* **56**, 4822 (1997)

Sloan, I., and S. Joe, "Lattice methods for multiple integration" Oxford Science Publications, New York 1994

Stephan, U., and D. Drabold, *Phys. Rev. B* **57**, 6391 (1998)

Stewart, J., P. Csaszar and P. Pulay, *J. of Comp. Chem.* **39**, 4997 (1982)

Stewart, J., *Int. J. of Quant. Chem.* **58**, 133 (1996)

Štich, I., R. Car, M. Parrinello, and S. Baroni, *Phys. Rev. B* **39**, 4997 (1989)

Strain, M., G. Scuseria and M. Frisch, *Science* **271**, 51 (1996)

Stratmann, R., G. Scuseria and M. Frisch, *Chem. Phys. Lett.* **257**, 213 (1996)

Strout, D., and G. Scuseria, *J. Chem. Phys.* **102**, 8448 (1995)

Szabo, A. and N. Ostlund "Modern Quantum Chemistry" McGraw Hill, New York, 1982

Teter, M., M. Payne, and D. Allan, *Phys. Rev. B* **40**, 12255 (1989)

Voter, A., J. Kress and R. Silver, *Phys. Rev. B* **53**, 12733 (1996)

Wang, L.-W., and M. Teter, *Phys. Rev. B* **46**, 12798 (1992)

Wang, L.-W., *Phys. Rev. B* **49**, 10154 (1994)

Wang, Y., G. Stocks, W. Shelton D. Nicholson, Z. Szotek and W. Temmerman, *Phys. Rev. Lett.* **75**, 2867 (1995)

Weinert, M., and J. Davenport, *Phys. Rev. B* **45**, 11709 (1992)

Wentzcovitch, R., J. L. Martins and P. Allen, *Phys. Rev. B* **45**, 11372 (1992)

White, S., J. Wilkins and M. Teter, *Phys. Rev. B* **39**, 5819 (1989)

White, C., B. Johnson, P. Gill and M. Head-Gordon, *Chem. Phys. Lett.* **230**, 8 (1994)

White, C., P. Maslen, M. Lee and M. Head-Gordon, *Chem. Phys. Lett.* **276**, 133 (1997)

Wimmer, E., *Mater. Sci. Eng. B* **37**, 72 (1996)

Xu, C., and G. Scuseria, *Chem. Phys. Lett.* **262**, 219 (1996)

Yang, W., *Phys. Rev. Lett.* **66**, 1438 (1991)

Yang, W., *J. Chem Phys.* **94**, 1208 (1991)

Yang, W., and T-S. Lee, *J. Chem. Phys. Rev. B* **103**, 5674 (1995)

Yang, W., *Phys. Rev. B* **56**, 9294 (1997)

York, D., T-S. Lee and W. Yang, *J. Am. Chem. Soc.* **118**, 10940 (1996)

Zhao, Q., and W. Yang, *J. Chem. Phys.* **102**, 9598 (1995)

Zhou, S., D. Beazley, P. Lomdahl and B. Holian, *Phys. Rev. Lett.* **78**, 479 (1997)